Pergamon

Geochimica et Cosmochimica Acta, Vol. 67, No. 22, pp. 4353–4371, 2003

0016-7037/03 $30.00 + .00

doi:10.1016/S0016-7037(03)00370-3

Rb/Sr record of fluid-rock interaction in eclogites: The Marun-Keu complex, Polar Urals, Russia

JOHANNES GLODNY,[1,2,6,*] HÅKON AUSTRHEIM,[2] JOSÉ F. MOLINA,[2,3] ANATOLIJ I. RUSIN,[4] and DIANE SEWARD[5]

[1]GeoForschungsZentrum Potsdam, Telegrafenberg C2, 14473 Potsdam, Germany
[2]Inst. for Geologi, Universitetet i Oslo, Postboks 1047, Blindern, 0316 Oslo, Norway
[3]Dept. of Mineralogy and Petrology, Campus Fuentenueva, E-18002 Granada, Spain
[4]Institute of Geology and Geochemistry, Ubr RAS, Pochtovy Per. 7, Yekaterinburg 62015, Russia
[5]Departement für Erdwissenschaften, ETH Zentrum, 8092 Zürich, Switzerland
[6]Zentrallabor für Geochronologie, Institut für Mineralogie, Universität Münster, Corrensstr. 24, 48149 Münster, Germany

(*Received July* 2, 2002; *accepted in revised form May* 6, 2003)

Abstract—Rb/Sr internal mineral isochrons in the eclogite facies Marun-Keu metamorphic complex, Polar Urals, Russia, date periods of fluid-rock interaction and record the metamorphic reaction history. The Marun-Keu complex consists of Late Proterozoic to Early Ordovician, mostly igneous rocks that experienced a subduction-related, non-pervasive eclogite facies metamorphism, followed by a local decompression-related amphibolite facies overprint, during the Uralian orogeny. Field observations show that metamorphic reactions as well as ductile deformation are controlled by local availability of a free fluid phase. Isotopic data reveals that availability of fluids similarly exerts control on isotope distribution. From a relic gabbro which has never been infiltrated by free fluids, a premetamorphic Rb/Sr age of 467 ± 39 Ma was obtained. Rb/Sr isochron ages for 14 samples of eclogite and amphibolite facies assemblages, sampled from within or close to metamorphic fluid veins, range from 352 ± 5 Ma to 360 ± 3 Ma. A Sm/Nd isochron for a metagranite yields an age of 354 ± 4 Ma. Taken together, the ages for both prograde and retrograde metamorphic assemblages overlap within analytical uncertainty and yield an average value of 355.5 ± 1.4 Ma, indicating that the metamorphic evolution and incipient exhumation of the Marun-Keu complex proceeded rapidly. The results demonstrate that assemblages preserve their Rb/Sr isotopic signatures as long as they remain devoid of free fluids, and that only fluid-rock interaction may cause Sr isotope redistribution. In addition, the data suggest local fluid-rock equilibrium, low fluid-rock ratios with overall fluid deficiency, and limited fluid mobility at depth. However, some fluids must have been mobile on the km-scale since they can be traced into the suprasubduction zone mantle wedge. Metasomatic veins in the Rai-Iz ophiolite yield a Rb/Sr mineral isochron age of 373.1 ± 5.4 Ma. They are interpreted as evidence for suprasubduction zone metasomatism in an oceanic setting, prior to subduction of the East European margin and associated formation of eclogites in the Marun-Keu complex.

We propose that Rb/Sr mineral-isochron ages provide hygrochronological rather than thermochronological constraints. They define the cooling history only in combination with zircon and apatite fission track data. The straightforward interpretation of Rb/Sr mineral ages as cooling ages is obsolete. *Copyright © 2003 Elsevier Ltd*

1. INTRODUCTION

Eclogite facies rocks are indicative of transient high pressure/temperature conditions, and carry information on nature and velocity of orogenic processes at depth. The evolution of high-pressure complexes in terms of P-T, fluid-rock interaction, and deformation can be derived from isotopic data if precise and accurate ages can be attributed in a reliable way to the different evolutionary stages. To constrain the exact timing of eclogite facies events by geochronological methods is, however, considered to be difficult (e.g., Cliff et al., 1998). The present paper highlights the potential of Rb/Sr internal mineral isochrons for this purpose.

Phengite-based Rb/Sr internal mineral-isochron ages for high pressure rocks have, until recently, mostly been interpreted as cooling ages. With few exceptions (Stosch and Lugmair, 1990; Glodny et al., 2002), they were considered to directly date metamorphic processes only if crystallization took place at or below the commonly accepted closure temperature for white mica (ca. 550°C, e.g., Blanckenburg et al., 1989; Inger et al., 1996).

The widely used closure temperature concept of Dodson (1973; 1979) focuses on temperature-driven volume diffusion within an individual mineral grain for modeling its isotopic closure, and assumes infinitely effective isotope removal mechanisms outside the grain. This assumption is by far not always met. Dodson's (1979) first sentence in his outline of the theory is *"A datable mineral, such as biotite, is considered to be physically connected (probably through a fluid phase) with a very large reservoir or sink within which radiogenic isotopes can be effectively lost"*. However, in later application of the concept, the key role of grain boundary fluids was generally underestimated. In absence of a free fluid phase, apparently the classical theory of isotopic closure is not applicable, and the transport properties of the specific matrix assemblage must be considered.

A potential analogy to the kinetic role of fluids for isotope redistribution is the role of fluids in metamorphic reaction kinetics. In anhydrous rocks, the timing of metamorphic reac-

* Author to whom correspondence should be addressed (glodnyj@gfz-potsdam.de).

tions is controlled by the appearance of free fluids (Yardley and Baltatzis, 1985; Rubie, 1986, 1990; Austrheim et al., 1997; Ernst et al., 1998) rather than by the crossing of equilibrium boundaries in the P-T space, possibly except for reactions at very high temperatures. For high-pressure rocks, the indispensability of fluids for metamorphism has been pointed out for both prograde reactions (e.g., Rubie, 1990; Biino and Compagnoni, 1992; Austrheim et al., 1997; Markl and Bucher, 1997; Scambelluri et al., 1998; Engvik et al., 2000; Molina et al., 2002) and for retrograde overprints (Heinrich, 1982; Rubie, 1986; Markl and Bucher, 1997; Straume and Austrheim, 1999; Molina et al., 2002). Apparently, metamorphism (in the sense of physico-chemical reequilibration) is related to fluid presence or fluid infiltration.

In this paper we hypothesize that isotope redistribution and isotope reequilibration is, in the same way as metamorphism, related to fluid-rock interaction (and possibly to deformation), much more than to elevated temperatures alone. Such a close link between metamorphic reaction kinetics and isotope redistribution kinetics would mean that preservation of petrographic relics concurrently implies preservation of relic isotopic signatures, which could then be used do date separate metamorphic reactions in polymetamorphic complexes. Rb/Sr internal mineral isochrons should provide reaction ages, probably even for processes at temperatures in excess of the commonly accepted closure temperatures, instead of the age of cooling below an isotherm.

As a test for this hypothesis, we investigated Rb/Sr mineral systematics of samples reflecting all distinguishable metamorphic processes in the Paleozoic Marun-Keu eclogite facies complex, Polar Urals, Russia. This complex locally exhibits perfect preservation of protoliths (fluid deficient at all times), of eclogite facies assemblages (in particular in vicinity to eclogite facies fluid pathways) and of decompression-related amphibolite facies assemblages (in domains which had free fluids at amphibolite facies conditions). In addition, we analyzed the Sm/Nd systematics of some samples. Thermochronologic constraints come from zircon and apatite fission track data. To define a minimum age for incipient subduction in the Polar Urals paleosubduction system, we dated subduction-fluid-related veining in the Rai-Iz ophiolite complex, which forms part of an ophiolite nappe overlying the eclogites.

The objectives of this paper are a) to demonstrate that both prograde and retrograde metamorphic reactions in subducted rocks are fluid-mediated, and that Rb/Sr mineral systematics of fluid-controlled mineral assemblages can provide the ages for separate metamorphic reaction events even in high temperature environments, b) to demonstrate that the isotopic record of fluid-precipitated assemblages provides close constraints on sources and nature of fluids at depth, c) to decipher the tectonometamorphic evolution of the Polar Urals paleosubduction system, and d) to discuss general consequences for the interpretation of geochronological data, in particular of Rb/Sr internal mineral isochrons.

2. GEOLOGICAL FRAMEWORK

The Uralian orogenic belt formed by collision of the East European Platform with an assemblage of Siberian-Kazakhian terranes in Devonian to Triassic time (Hamilton, 1970, Zonenshain et al., 1984). The Main Uralian Fault, separating rocks of the East European Platform from microcontinents and island arcs further east, is the main suture zone of the orogen. Blueschist and eclogite facies metamorphic complexes crop out in a narrow, discontinuous, over 2000 km long belt along the western side, i.e., in the footwall of the Main Uralian Fault (Dobretsov and Sobolev, 1984; Sobolev et al., 1986). Among these complexes are the Maksyutov complex, Southern Urals (e.g., Ivanov et al., 1975; Glodny et al., 2002 and references therein) as well as the Nerkau complex, Northern Urals (e.g., Gomez-Pugnaire et al., 1997) and the Marun-Keu complex, Polar Urals (e.g., Udovkina, 1971; Sobolev et al., 1986; Molina et al., 2002). There are striking similarities between these complexes regarding metamorphic grade, internal structure and tectonic position (Sobolev et al., 1986; Lennykh et al., 1997; Puchkov, 1997).

The Marun-Keu complex is a lens-shaped body that trends NNE-SSW, along the main axis of the Uralian orogen (Fig. 1). It extends over an area of ca. 300 km^2, with a maximum NNE-SSW elongation of $\sim$ 60 km, and was metamorphosed at blueschist- to eclogite facies conditions. The complex is bounded to the west by a succession of latest Neoproterozoic (?) to Early Paleozoic greenschist facies metasediments (Udovkina, 1971; Bogdanov et al., 1996). Its eastern limit is the Main Uralian Fault, juxtaposing the complex beneath the ophiolitic Syum-Keu complex, the rocks of which grade towards E into island arc lithologies.

The present regional geological setting was assembled during Uralian, E-directed subduction of the East European passive margin (Savelieva and Nesbitt, 1996) and corresponding obduction of oceanic lithosphere. The exact timing of the Uralian processes has not yet been well constrained. The Syum-Keu ophiolite complex (Fig. 1) once formed a continuous nappe together with the Voykar/Rai-Iz ophiolites, approx. 100 km further south (Bogdanov et al., 1996). For the latter, a Sm/Nd study by Sharma et al. (1995) showed that the mantle rocks experienced extraction of basaltic melts at 387 $\pm$ 34 Ma (2σ errors given here and below).

The Marun-Keu complex represents metamorphosed continental crust of the East European craton, in the same way as the Maksyutov complex in the southern Urals (cf. Hetzel, 1999). Protoliths of the Marun-Keu complex are volcanic and plutonic rocks, intercalated with minor amounts of metasediments, which were formed in Neoproterozoic III to Early Ordovician times (Glodny et al., 1999). Among the (meta)igneous rocks, granitoids predominate but intermediate to gabbroic intrusives occur as well, constituting a wide range of bulk compositions and lithologies in the complex.

3. PETROGRAPHY OF METAMORPHIC PROCESSES

3.1. Eclogite: Terminology

The term "eclogite" is commonly used for rocks that contain the assemblage garnet + omphacite and are basaltic in bulk composition (e.g., Coleman et al., 1965; Carswell, 1990). Variable terminologies exist for cofacial felsic rocks. In this study, "eclogite" is used sensu lato, i.e., the term also comprises rocks of non-basaltic composition which show eclogite facies equi-

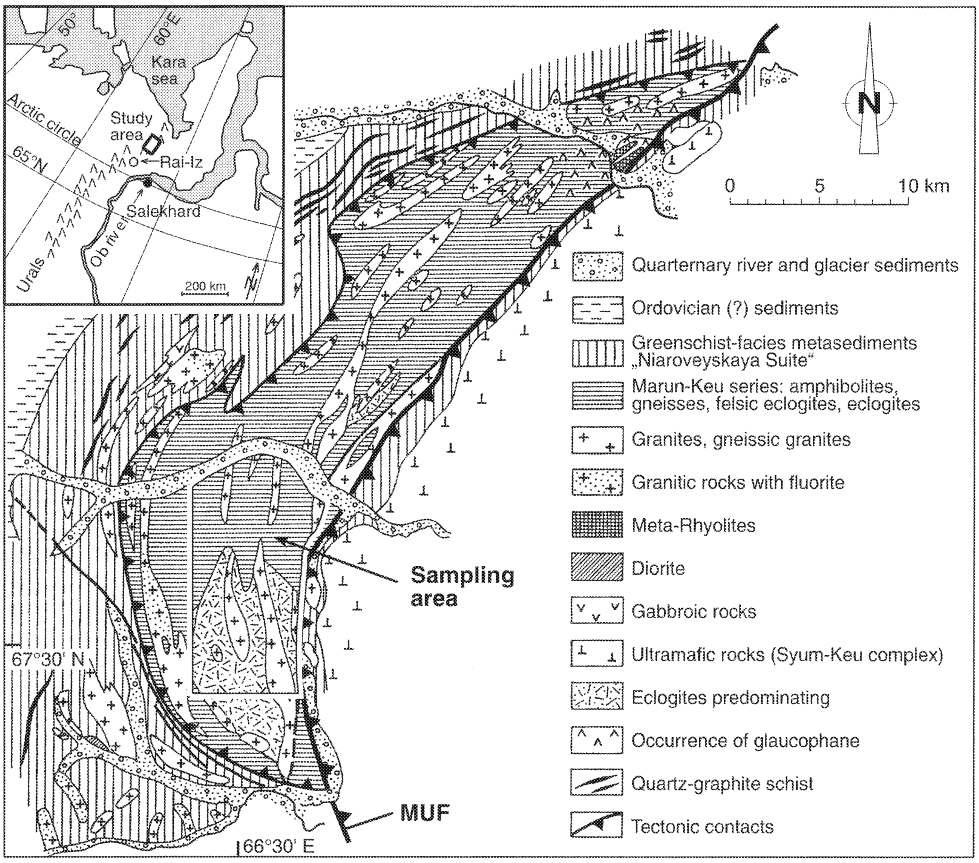

Fig. 1. Geological and tectonic map (modified after Udovkina, 1971) of the Marun-Keu complex, in the Polar part of the Urals mountain belt (see inset). MUF: Main Uralian Fault. Box identifies the study area in the southern part of the complex.

librium assemblages. We use the adjectives "eclogitic" and "eclogite facies" for detailed characterization of such rocks.

3.2. Protoliths and Metamorphic Processes in the Marun-Keu Complex

The effects of eclogite facies metamorphism in the Marun-Keu can be seen in a wide variety of protolith compositions which together are exemplary for continental crust. The recorded metamorphic conditions are variable both at the scale of the entire complex and at the outcrop scale. The northernmost part ("Pike river complex" of Sobolev et al., 1986) experienced metamorphic conditions of ca. 10–11 kbar, 500 °C (Dobretsov and Sobolev, 1984). In the southern part, which is the study area for the present work, metamorphic conditions between 14 and 17 kbar, 520–690°C are recorded (Udovkina, 1971; Molina et al., 2002). This fairly broad range in the study area is interpreted to be due to fluid-mediated equilibration at different stages of the metamorphic evolution (Molina et al., 2002).

Apart from abundant well-preserved high-pressure rocks, pre and early metamorphic relics occur, as well as retrogression-related assemblages. An outline of the petrological evidence for the metamorphic evolution is given below. Additional information can be found in Molina et al. (2002).

Protolith relics. Some gabbro domains survived the high-grade metamorphic conditions in a virtually undeformed and unreacted state. These domains are confined by partially to completely eclogitized zones which are related to local fluid pathways, scaled from major cracks down to grain boundaries. As an example, sample PU62 (Fig. 2a) presents a transition from virtually unreacted to completely eclogitized gabbro. Availability of fluids was the limiting factor for the eclogitization reactions (cf. Molina et al., 2002). Reaction ceased when the fluids were consumed by formation of hydrous eclogite facies phases (zoisite/epidote, barroisite). Analogous observations and conclusions were made for similar protolith-eclogite transitions elsewhere (e.g., Thöni and Jagoutz, 1992; Austrheim, 1998). Felsic igneous relic assemblages were not observed. However, some felsic rocks locally show relic igneous phases, like allanite or K-feldspar.

Protolith textures are frequently preserved, since eclogite facies deformation was confined to distinct, fluid-bearing shear zones. Significant posteclogite facies ductile deformation is not observed. Most protolith textures are magmatic in origin like e.g., mafic enclaves in granitoids (e.g., Vernon, 1984) which occur on the scale of cm to m. In some former subvolcanic and granitoid rocks the distribution of the fine-grained eclogite facies minerals mimics originally porphyric or equigranular textures.

Eclogite facies veins of different types are abundant. They are apparently randomly oriented in strike, often sinuous, and

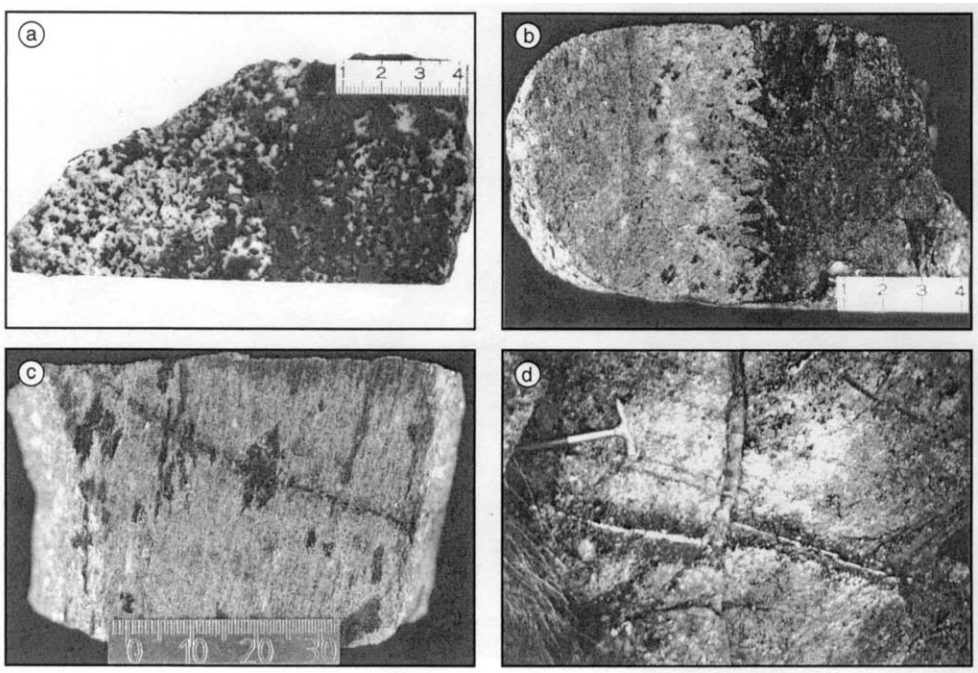

Fig. 2. Rocks documenting fluid-rock interaction. a) Sample PU62. Partially eclogitized gabbro. Reaction progress is low to the left (almost preserved gabbro) and high to the right (almost complete eclogitization). Note corona textures in the central part. Scale bar: cm. b): Sample J12. Quartz-phengite vein (to the left, mostly broken off), with reaction zone. Sheared eclogite to the left (J12a), undeformed eclogite with amphibole crystals in the central part (J12b), and garnet amphibolite (J12c) to the right. Scale bar: cm. c): Sample PU55. Eclogite, with amphibole megablasts, cut by a tiny retrogressive fluid vein. Amphibole megablast growth is not related to retrogression. Scale bar: mm. d): Fracture system, with fluid-induced amphibolitization (dark bands) of eclogite. Note feldspar vein in the center of one of the amphibolitization zones. Hammerhead (13 cm) for scale.

reach thicknesses between <1 mm and ~ 20 cm. The veins are localized features, an interconnected fracture system is not evident. Their mineralogy is variable but quartz-rich veins predominate, with phengite, paragonite, omphacite, garnet, apatite (often Cl-rich) and rutile as accessory minerals. Other veins are dominated by grossular-andradite $\pm$ diopside. Almost monomineralic omphacite or garnet veins occur as well. Some veins show symmetrical banding, e.g., a quartz-rich central part, rimmed by an omphacite domain which grades into the wall rock. Typically the veins either contain garnet + omphacite, or this assemblage is present and stable in the immediate wall rock, indicating presence of fluids during eclogite facies conditions. Many veins are accompanied by alteration/reaction haloes in the wallrock, characterized e.g., by increasing modal abundance of omphacite and grain coarsening (Fig. 2b), or by increasingly abundant growth of dendritic amphibole towards the fluid pathway (Fig. 3b). These textural relationships suggest that wallrock eclogitization was mediated by fluids.

There is a strong spatial correlation between eclogite facies fluid pathways and deformation. In many cases strain was either partitioned into the fluid pathway mineralizations or into the immediate wallrocks, generating strongly foliated eclogites.

Eclogite facies rocks have assemblages which depend on both the whole rock chemistry and on the actual P,T,X conditions during crystallization. P,T conditions between 14–17 kbar and 520°–690°C, respectively, are recorded (Molina et al., 2002). Mafic eclogites consist of garnet + omphacite + phengite (up to 3.36 apfu Si) + Ca-Na-amphibole. Felsic, SiO_2-rich lithologies are dominated by quartz, phengite, zoisite/clinozoisite, K-feldspar, minor omphacite and garnet and, in places, plagioclase. Plagioclase (generally Ab_{80-100}) stability depends on the local chemical environment. In some metagranitoids, plagioclase is transformed into fine-grained aggregates of zoisite-epidote-phengite-albite, in others it is in textural equilibrium with omphacite. Plagioclase stability was shown to be characteristic for felsic eclogite facies rocks (Klemd and Bröcker, 1999). Some eclogites exhibit skeletal, "dendritic," poikiloblastic amphibole crystals up to 1 cm in diameter. Microtextures and mass balance calculations suggest that they formed at eclogite facies conditions, in presence of fluids (Fig. 2c). *Eclogite textures* are variable. Some samples exhibit prograde fabrics, like high-pressure foliation defined by phengite and omphacite. Other samples show equilibrium crystallization textures.

The retrograde veins are straight, generally undeformed veins of up to 0.2 m in diameter, filled with coarse-grained plagioclase $\pm$ K-feldspar, quartz, white mica, $\pm$ amphibole $\pm$ epidote. Apparently they occur only in mafic lithologies. The veins follow mesoscopic to macroscopic fracture systems and are surrounded by mm- to dm-wide hydrated zones (Figs. 2c,d) in which eclogite is transformed to amphibolite facies mineral associations. The veins, together with micro-cracks, act as fluid pathways supplying fluids which induce retrogression of the wallrock, as similarly observed in other eclogite facies complexes (e.g., Selverstone et al., 1992; Straume and Austrheim, 1999).

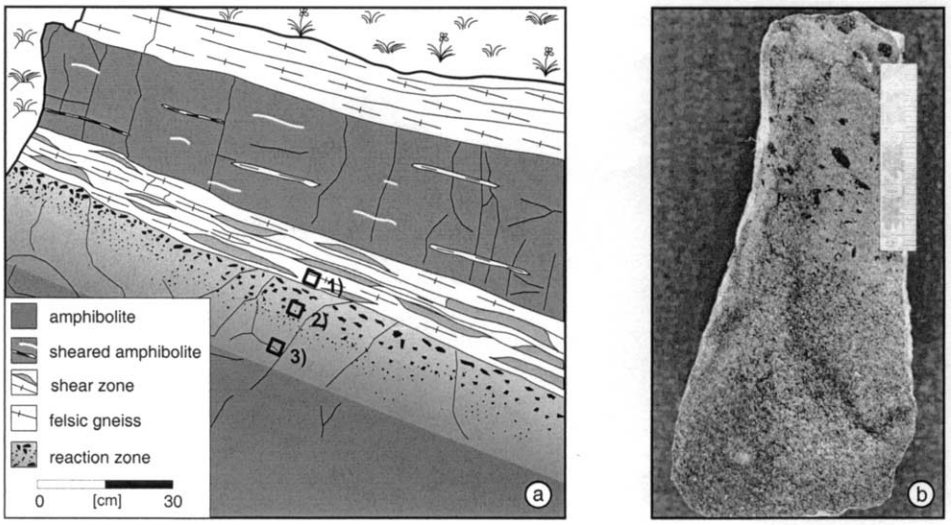

Fig. 3. Outcrop situation for samples J30/J32. a) Shear zone. Wallrock is eclogite near the shear zone, and garnet amphibolite further away. Reaction is due to fluid infiltration normal to the shear axis. Origin of samples: 1): J30. 2): J32a (eclogite). 3): J32c (transition zone). b) Detail of the reaction zone, with amphibole megablasts in the upper part of the sample, close to the shear zone. Scale bar: mm.

Retrogression of the eclogites occurred at amphibolite facies conditions. Indications for local greenschist facies overprint are rare. Calcic amphibole, plagioclase, biotite and, locally, "smaragdite" (Cr-amphibole) grew at the expense of omphacite, phengite and Na-Ca-amphibole; rutile was replaced by sphene. Biotite forms conspicious small epitactic overgrowths on phengite. To constrain the metamorphic conditions of retrogression is generally difficult. However, retrogression in sample PU31 (see Tables 1, 2 and Appendix) took place between 12 and 8 kbar, as inferred by unstability of omphacite and stability of garnet (cf. Poli, 1993). In this sample, amphiboles are barroisite in the cores and magnesio-hornblende in the rims. Plagioclase is nearly pure albite (X Ab = 0.98–1.00). Using the amphibole-plagioclase thermometer of Holland and Blundy (1994), temperatures between 535° and 575°C are calculated for the retrogression reactions (Table 1). Garnet is present in most retrogression environments, in places as relic garnet that contains omphacite and phengite inclusions. The retrogression took place mainly at static conditions; ductile shearing at amphibolite facies conditions is only locally observed.

3.3. Vein Assemblages in the Rai-Iz Complex. Subduction Fluids?

The ultramafic Rai-Iz complex, an equivalent to the Syum-Keu ophiolite, that tectonically overlies the Marun-Keu eclogites, is interpreted to represent part of the suprasubduction zone mantle wedge. Structure and lithologies of the Rai-Iz complex have been described in detail elsewhere (Shmelev and Puchkov, 1986; Garuti et al., 1999). Here, mantle rocks, like chromite-rich dunites and lherzolites, are locally crosscut by cm- to *m*-wide veins, consisting of plagioclase (albite) + amphibole + chromite + phlogopite + corundum (ruby) ± apatite. A tectonic setting of extension and exhumation of the ophiolite at crustal depths of less than 30 km during vein formation is indicated by I) mineralization of extensional fractures, II) by widespread serpentinization in the respective wallrocks, and III) the abundance of albite (cf. Johnson and Harlow 1999). The age of vein formation therefore may place a minimum age for the onset of subduction in the Polar Urals and for incipient obduction of the ophiolites.

4. SAMPLING STRATEGY AND ANALYTICAL PROCEDURES

For Rb/Sr isotope work, we separated minerals from small (<100g), lithologically homogeneous samples to avoid sampling of larger-scale Sr-isotopic heterogeneities (Glodny et al., 2002). Most importantly, for retrieving eclogite facies (or generally high temperature) Sr isotope information it is essential to sample exclusively unretrogressed assemblages, as discussed below. We intended to analyze, whenever possible in replicate, material formed specifically during the different discriminable stages of the metamorphic evolution. The detailed petrography of the samples is summarized in the appendix.

For Rb/Sr and Sm/Nd isotope analyses, pure mineral separates of all major Sr-bearing phases of a rock were produced. Mica fractions were ground in ethanol in an agate mortar and then sieved in ethanol to obtain inclusion-free separates. Secondary (Fe, Mn)-hydroxides on some omphacite and garnet separates were removed with a 5% aqueous solution of oxalic acid. Whole rock powders were prepared in an agate mill. For isotope data obtained at the Potsdam and Oslo laboratories, an outline of analytical procedures and the results of standard analyses are presented in Glodny et al. (2002); for the data generated at Münster University, details are given in Glodny et al. (1998). For age calculations, 2σ standard errors of ± 0.005% for $^{87}Sr/^{86}Sr$ ratios, ± 1.5% for $^{87}Rb/^{86}Sr$, ± 0.003% for $^{143}Nd/^{144}Nd$, and ± 0.5% for $^{147}Sm/^{144}Nd$ ratios were assigned to the results if analytical errors were smaller than these values. The program ISOPLOT/EX 2.06 (Ludwig, 1999) was used to calculate regression lines. Analytical details for the

Table 1. Amphibole analyses, T estimates.

Label Textural position	PU31a-5 rim	PU31a-6 core
wt.%		
SiO_2	45.86	46.74
TiO_2	0.33	0.30
Al_2O_3	11.38	10.71
Cr_2O_3	0.09	0.13
NiO	0.00	0.00
FeO	13.50	12.33
MnO	0.14	0.17
MgO	10.75	11.61
CaO	10.14	10.67
Na_2O	2.21	1.99
K_2O	0.61	0.58
Total	95.01	95.24
Si	6.855	6.951
Ti	0.037	0.034
Al	2.003	1.874
Cr	0.010	0.016
Ni	0.000	0.000
Fe	1.685	1.531
Mn	0.018	0.021
Mg	2.392	2.570
Ca	1.621	1.698
Na	0.639	0.573
K	0.117	0.110
Fe^{3+}	0.313	0.135
Fe^{2+}	1.372	1.396
Al^{IV}	1.145	1.049
Al^{VI}	0.858	0.825
Na^{M4}	0.379	0.302
Na^{A}	0.260	0.271
XAb (plagioclase)	0.989	0.989
XV	0.623	0.619
XNa M4	0.190	0.151
XAl M2	0.429	0.412
XSi T1	0.714	0.738
XAl T1	0.286	0.262
T (°C), at 12 kbar	573	562
T (°C), at 10 kbar	559	549
T (°C), at 8 kbar	544	536

Amphibole analyses for amphibolite of sample PU31, and amphibole-plagioclase temperature estimates after Holland and Blundy (1994). Cations per 23 oxygen. Additional analyses from this and other samples are presented in Molina et al. (2002). Amphibole compositions were obtained on a Cameca Camebax electron microprobe (wavelength dispersive system) at the Mineralogical-Geological Museum, Oslo University, using natural and synthetic standards. Acceleration voltage was fixed to 15 kV, at a beam current of 20 nA.

zircon and apatite fission track data are given in Seward et al. (2002).

5. RESULTS

The results of Rb/Sr analyses of mineral separates and whole rock powders of rocks from the Marun-Keu and Rai-Iz complexes are presented in Table 2. Selected results are displayed as isochron plots in Figure 4. Two samples of eclogite (PU12 and PU22) were analyzed for evaluation of Sm/Nd systematics. Results are listed in Table 3. The Marun-Keu protolith sample PU62 yields an Rb/Sr isochron age of 467 ± 39 Ma. The Rb/Sr and Sm/Nd isochron ages for eclogite facies veins, eclogites, retrogression-related veins and retrogressed eclogites of the Marun-Keu complex all fall in a very narrow range, between 360.0 and 351.1 Ma (Fig. 5). The age error intervals overlap. Calculation of average ages yields 356.1 ± 1.4 Ma (MSWD = 1.6, average weighted by individual errors) or 355.5 ± 1.4 Ma (Tukey's Biweight Mean). The vein assemblage from the ophiolitic Rai-Iz complex is clearly older, and has a Rb/Sr isochron age of 373.1 ± 5.4 Ma.

For age calculation, certain analytical data were excluded for the following reasons: In sample J 12, the data for amphibole J12c is regarded as an outlier. In sample J 13, the amphibolite whole rock is apparently weathered. The same applies for the J25 whole rock. Apatite of sample J24 has an altered ("silky") appearance. For sample PU10a, biotite-apatite-regression was calculated because apatite exhibits the most primitive Sr isotopic composition, i.e., apatite is the least altered material in this rock. Sample PU12 shows alteration, in particular chloritization of biotite. Consequently, biotite and whole rock data are regarded as aberrant.

To detect possible metasomatism in the rocks subjected to fluid-rock interaction, we studied the elemental chemistry of some fluid-induced lithological transitions. In addition, rock densities were determined. Results are given in Table 4. Zircon and apatite fission track data are presented in Table 5.

6. DISCUSSION

6.1. Rb/Sr Mineral Isochrons: Crystallization or Cooling Ages?

The key issue in the interpretation of Rb/Sr mineral data is as to whether an isochron age reflects crystallization of an assemblage, or cooling through a closure temperature. The regional metamorphic temperatures in the Marun-Keu complex reached 520–690°C during eclogite facies, with retrogression to amphibolite facies at 535–575°C. Following commonly held views, these temperatures lie close to or above the closure temperature for Rb/Sr in white mica (many estimates in the range of 500–550°C, e.g., Blanckenburg et al., 1989 and references therein; Inger et al., 1996). Hence, the ages obtained from white mica-bearing assemblages would be cooling ages. However, this interpretation is problematic since both Rb/Sr biotite ages and Sm/Nd garnet-whole rock ages are identical to the Rb/Sr white mica ages (Table 2), despite the considerably different "closure temperatures" of the respective systems.

Since ages in isochron-based geochronological systems reflect events of isotopic homogenization, valid ages can only be obtained for geological events which enabled isotope transport between different reservoirs (e.g., minerals, fluid) in a rock. Therefore, kinetic aspects are of crucial importance for the interpretation of Rb/Sr mineral isochron data. If isotope transport and intergranular isotope exchange in a rock is inhibited, the actual temperature is not relevant, and radiogenic Sr will remain locked in place because there is no place to which it could diffuse. In case of such unfavourable isotope transport kinetics, obviously the classical theory of isotopic closure is not applicable.

Free aqueous fluids play a key role for element and isotope transport kinetics in a rock. In absence of fluids, minerals have

Table 2. Rb/Sr analytical data.

Sample No. Analysis No.	Material	Rb [ppm]	Sr [ppm]	$^{87}Rb/^{86}Sr$	$^{87}Sr/^{88}Sr$	$^{87}Sr/^{88}Sr$ $2\sigma_m$ [%]
Partially preserved igneous protolith assemblages						
PU62 (467 ± 39 Ma, MSWD = 0.32, Sr_i = 0.704923 ± 0.000032)						
PS457	amphibole/clinopyroxene	0.50	14.69	0.0989	0.705582	0.0014
PS506	plagiodase	2.58	445.9	0.0167	0.705041	0.0012
PS469	whole rock	1.91	222.0	0.0249	0.705081	0.0014
Eclogite facies veins/shear zones and related prograde metamorphism						
J2 (356 ± 4 Ma, MSWD = 0.68, Sr_i = 0.706131 ± 0.000025)						
OS69	white mica (vein)	342.8	714.2	1.3893	0.713224	0.0024
OS70	apatite (eclogite)	0.08	2601	0.0001	0.706135	0.0012
PS453	white mica (eclogite)	355.7	559.9	1.8393	0.715406	0.0020
OS68	omphacite (eclogite)	0.26	48.63	0.0157	0.706206	0.0022
J13 (351.1 ± 6.9 Ma, Sr_i = 0.709174 ± 0.000054)						
PS458	white mica > 500 μm, vein	288.0	560.1	1.4886	0.716614	0.0014
PS459	omphacite-concentrate	7.65	84.57	0.2617	0.710482	0.0016
PS460	amphibolite whole rock*	3.11	183.4	0.0490	0.709545	0.0014
J21 (357.3 ± 6.6 Ma, Sr_i = 0.705440 ± 0.000047)						
OS26	white mica 0.6 cm	271.5	522.4	1.5045	0.713093	0.0025
OS27	whole rock	22.38	331.9	0.1950	0.706432	0.0038
J30, J32 (J30 only: 353.3 ± 3.1 Ma, MSWD = 1.2, Sr_i = 0.706295 ± 0.000027)						
OS66	J30 amphibole	1.84	45.37	0.1176	0.706938	0.0100
OS52	J30 white mica > 500 μm	239.5	256.9	2.7000	0.719896	0.0026
PS157	J30 wm > 500 μm rep.	248.6	266.6	2.7016	0.719899	0.0018
PS463	J30 apatite	0.53	1011	0.0015	0.706309	0.0014
PS452	J30 wm 100–200 μm	242.2	254.4	2.7581	0.720185	0.0014
OS51	J30 whole rock	48.00	436.1	0.3184	0.707864	0.0014
PS483	J32 wr 15 cm from sz	50.13	80.00	1.8144	0.715336	0.0012
PS484	J32 wr 3 cm from sz	53.94	54.49	2.8674	0.720692	0.0012
Eclogite facies equilibrium assemblages						
J12 (360.0 ± 2.6 Ma, MSWD = 0.69, Sr_i = 0.706524 ± 0.000018)						
OS72	12 a omphacite	2.25	78.20	0.0834	0.706932	0.0012
OS14	12 a wm 125–250 μm	359.5	866.4	1.2013	0.712642	0.0014
OS15	12 a wm > 500 μm	375.1	800.6	1.356	0.713489	0.0022
PS476	12 a apatite	0.12	2595	0.0001	0.706540	0.0012
OS18	12 a whole rock	118.5	378.5	0.9058	0.711169	0.0026
OS13	12 b wm 250–500 μm	365.3	1011	1.0457	0.711911	0.0025
OS50	12 b omphacite	0.54	71.98	0.0216	0.706643	0.0030
OS17	12 b whole rock	61.58	201.5	0.8845	0.711014	0.0014
OS12	12 c wm 250–500 μm	395.8	799.7	1.4327	0.713941	0.0018
PS477	12 c apatite	0.67	5355	0.0004	0.706527	0.0014
OS71	12 c amphibole*	7.13	114.9	0.1796	0.707331	0.0010
OS16	12 c whole rock	30.36	173.5	0.5063	0.709112	0.0024
J24 (355.7 ± 3.2 Ma, MSWD = 1.16, Sr_i = 0.707570 ± 0.000012)						
PS599	white mica > 500 μm	352.8	207.4	4.9341	0.732613	0.0012
PS455	white mica 250–100 μm	346.1	199.3	5.0357	0.732942	0.0012
OS48	plagioclase I	0.65	590.4	0.0032	0.707583	0.0027
PS601	plagioclase II	0.92	608.9	0.00437	0.707579	0.0014
PS621	garnet, leached	1.27	45.47	0.0807	0.707996	0.0016
PS622	apatite*	1.40	621.5	0.0065	0.707706	0.0016
OS30	whole rock	69.88	363.7	0.5561	0.710385	0.0030
J25 (355.2 ± 3.9 Ma, MSWD = 0.85, Sr_i = 0.708051 ± 0.000036)						
AS10135	amphibole	6.88	37.67	0.5281	0.710702	0.0052
AS10131	white mica > 710 μm	364.2	296.0	3.5666	0.726114	0.0025
AS10132	white mica 250–160 μm	374.4	247.8	4.3814	0.730222	0.0025
PS467	omphacite 2	2.56	41.43	0.1785	0.708968	0.0014
AS10137	omphacite 1	1.10	25.20	0.1266	0.708603	0.0209
AS10138	whole rock*	19.54	300.3	0.1883	0.709102	0.0028

(Continued)

been shown to preserve their Sr, O, Ar-isotopic signatures through temperatures far above their commonly accepted closure temperatures, even for timescales of entire metamorphic episodes (Farquhar et al., 1996; Tilton et al., 1997; Kelley and Wartho, 2000; Kühn et al., 2000). Petrologic equilibria are metastably preserved as well: In absence of free fluids, equilibrium reaction boundaries are overstepped, and preexisting assemblages are preserved as petrographic relics. Theoretical considerations by Ahrens and Schubert (1975) indicate that, at eclogite facies conditions with temperatures from 600°C to 800°C but in absence of free fluids, transformation from gabbro to eclogite would not occur in geologically reasonable times.

Table 2. (Continued)

Sample No. Analysis No.	Material	Rb [ppm]	Sr [ppm]	$^{87}Rb/^{86}Sr$	$^{87}Sr/^{88}Sr$	$^{87}Sr/^{88}Sr$ 2σm [%]
PU55 (356.4 ± 3.2 Ma, MSWD = 2.4, Sr_i = 0.706480 ± 0.000042)						
PS617	white mica nm 0.9 A	367.2	384.6	2.7657	0.720510	0.0012
PS618	white mica > 500 μm	371.2	357.0	3.0117	0.721732	0.0012
PS619	white mica m 0.8–0.9 A	369.2	380.4	2.8114	0.720644	0.0012
PS630	white mica m 0.7 A	367.0	372.9	2.8513	0.720926	0.0014
PS631	white mica m 0.7–0.8 A	363.3	377.5	2.7886	0.720747	0.0012
PS629	amphibole	10.02	50.34	0.5760	0.709431	0.0014
PS632	apatite	5.76	1397	0.0119	0.706560	0.0014
PS620	omphacite	1.64	31.81	0.1488	0.707193	0.0034
PU61 (352.0 ± 4.9 Ma, MSWD = 0.37, Sr_i = 0.704795 ± 0.000021)						
PS296	biotite	299.7	72.04	12.105	0.765484	0.0016
PS325	apatite	0.11	7650	0.0000	0.704807	0.0018
PS306	omphacite	0.32	203.0	0.0046	0.704809	0.0016
PS358	whole rock	9.43	120.8	0.2257	0.705924	0.0016
Retrogression (amphibolitization) related veins and retrogressed rocks						
J5 (357.9 ± 3.7 Ma, MSWD = 0.35, Sr_i = 0.706866 ± 0.000035)						
PS466	plagioclase	12.81	1197	0.0310	0.707024	0.0018
PS470	white mica 3 × 7 mm	288.1	103.3	8.0961	0.748249	0.0018
PS454	white mica 1 × 5 cm	289.5	102.1	8.2381	0.748709	0.0016
PU10a (biotite-apatite age: 357.6 ± 5.2 Ma; Sr-isotopic disequilibria)						
OS20	whole rock	165.5	22.65	21.432	0.849738	0.0060
OS19	green biotite	652.9	4.17	587.82	3.739124	0.0042
PS461	apatite	1.70	182.7	0.0271	0.746647	0.0014
OS25	epidote	12.38	636.3	0.0565	0.749341	0.0023
PU12 (353 ± 6 Ma, MSWD = 2, Sr_i = 0.723641 ± 0.000047)						
OS40	plagioclase	0.73	193.1	0.0110	0.723664	0.0023
PS456	white mica 250–100 μm	395.1	168.9	6.7993	0.757728	0.0014
OS41	muscovite 250–500 μm	399.4	187.7	6.1646	0.754666	0.0025
PS462	sphene	2.73	474.4	0.0167	0.723728	0.0016
PS464	apatite	0.63	5409	0.0003	0.723672	0.0016
OS42	biotite 250–500 μm*	670.8	23.05	86.534	0.991357	0.0023
OS43	whole rock*	96.88	138.7	2.0261	0.733504	0.0028
J22 (355.5 ± 5.1 Ma, MSWD = 0.3, Sr_i = 0.705267 ± 0.000029)						
AS10126	amphibole	9.23	88.75	0.3010	0.706782	0.0028
AS10127	white mica ca. 1 cm	494.6	461.1	3.1080	0.721021	0.0022
AS10128	clinozoisite/epidote	0.12	4048	0.0001	0.705273	0.0030
PU31 (357.9 ± 4.7 Ma, MSWD = 3.6, Sr_i = 0.704294 ± 0.000039)						
AS10139	omphacite (eclogite)	4.14	89.83	0.1333	0.704955	0.0110
PS602	amphibole (amphibolite)	7.04	29.13	0.6994	0.707841	0.0016
AS10130	white mica (eclogite)	272.9	308.4	2.5624	0.717365	0.0030
PS603	white mica (amphibolite)	373.1	283.7	3.8109	0.723803	0.0016
OS46	apatite (amphibolite)	2.27	172.1	0.0382	0.704518	0.0029
PS625	apatite (eclogite)	0.17	928.0	0.0005	0.704364	0.0012
AS10135	whole rock (eclogite)	15.39	178.9	0.2489	0.705539	0.0026
OS32	wr ecl-amphibolite trans.	13.06	176.9	0.2135	0.705360	0.0030
OS33	whole rock (amphibolite)	13.28	178.9	0.2147	0.705341	0.0030
Amphibolite- to greenschist facies overprint						
PU12 (see above for data: biotite/chlorite-whole rock date: 214.6 ± 3.2 Ma)						
PU32 (347.0 ± 5.1 Ma, Sr_i = 0.710602 ± 0.000045)						
PS35	omphacite	8.99	93.98	0.2769	0.711970	0.0024
PS37	biotite	881.1	5.20	642.76	3.88560	0.0010
Rai-lz ophiolite complex: vein mineralization						
PU4 (373.1 ± 5.4 Ma, MSWD = 0.42, Sr_i = 0.704817 ± 0.000019)						
AS10136	whole rock	15.17	5178	0.0085	0.704846	0.0030
AS10134	phlogopite	96.31	1250	0.2229	0.706011	0.0025
PS70	feldspar	2.19	7791	0.0008	0.704829	0.0014
PS86	amphibole	1.91	222.1	0.0248	0.704951	0.0016
PS58	phlogopite 2	125.9	166.4	2.1917	0.716449	0.0014

Errors are reported at the 2 σ level. (*): not used for age calculation. An uncertainty of ± 1.5 % has to be assigned to Rb/Sr ratios. rep.: replicate analysis; wm: white mica; wr: whole rock; sz: shear zone; ecl: eclogite; trans.: transition; m/nm: magnetic/nonmagnetic on Frantz magnetic separator, 13° tilt, at electric current as indicated. Analysis numbers indicate data origin: O . . . : Oslo University; P. . .: GeoForschungsZentrum Potsdam; A. . .: Münster University.

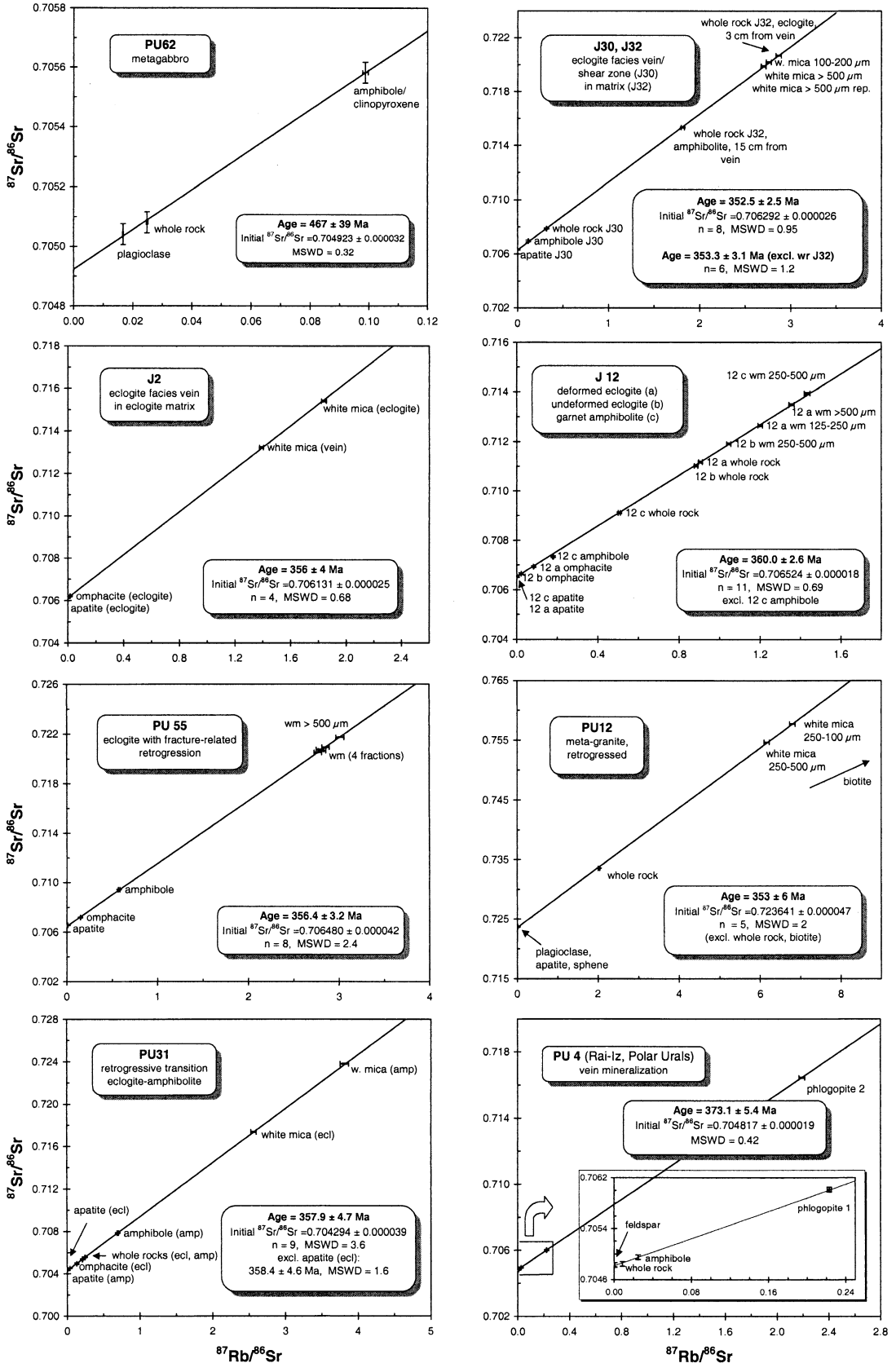

Fig. 4. Selected Rb/Sr isochron diagrams, Marun-Keu and Rai-Iz complexes, Polar Urals.

Table 3. Sm/Nd analytical data.

Sample	Material	Sm [ppm]	Nd [ppm]	$^{147}Sm/^{144}Nd$	$^{143}Nd/^{144}Nd$	$^{143}Nd/^{144}Nd$ $2\sigma_m$ [%]	εNd [380 Ma]
Rai-lz and Voikar ultramafic complexes							
PU4 (vein material; 361 ± 140 Ma, Nd_i = 0.512327 ± 0.000059)							
PS384	whole rock	0.0761	0.9197	0.0500	0.512445	0.0016	+3
PS391	amphibole	0.7001	5.7781	0.0733	0.512500	0.0014	
For comparison: Ultramafic rocks (Sharma et al., 1995):							+8.6
Marun-Keu metamorphic rocks							
PU12 (meta-granite; 354 ± 4 Ma; Nd_i = 0.511805 ± 0.000018)							
PS149	whole rock	3.3282	10.996	0.1830	0.512229	0.0030	
ON6	garnet	5.5853	2.9825	1.1410	0.514447	0.0040	
PU22 (meta-granite; Disequilibria, no age information)							
OS31	whole rock	6.8868	36.146	0.1160	0.512419	0.0022	
ON5	garnet	0.6470	3.2238	0.1222	0.512397	0.0029	
OS39	zoisite	185.17	807.61	0.1396	0.512450	0.0021	

Errors are reported at the 2 σ level. An uncertainty of ± 0.5 % has to be assigned to Sm/Nd ratios. Key to analysis numbers: see Table 2

Field evidence in eclogite facies complexes substantiates these considerations as commonly rocks with different equilibrium assemblages (unreacted protoliths, eclogites, and retrograde greenschist- or amphibolite facies assemblages) occur in short distance from each other, indicating that local assemblages are controlled by multiple subsequent local fluid-rock interaction episodes at different ambient P,T conditions. The importance of fluids for isotope systematics and petrology is due to their multifunctional role in a rock system. They are a phase which may exchange components or isotopes with minerals, they act as catalyst or component for metamorphic reactions, and they mediate transport processes, as diffusion through a fluid phase is very much more rapid than through crystalline silicates.

Therefore, for the interpretation of Rb/Sr mineral isochron data it is crucial a) to evaluate the contrasting isotope exchange kinetics among minerals at fluid-present and fluid-absent conditions and b) to distinguish periods of fluid-rock-interaction during the metamorphic history from periods of fluid absence. This approach opens the possibility to correlate age data directly with petrological processes documented in the rock.

In presence of a continuous intergranular fluid film, the mass transfer capacity of the intergranular space is expected to be high (e.g., Nakashima, 1995). In this case fluids may mediate isotope exchange even between non-adjacent grains. Therefore, in presence of fluids, the mineralogical composition of the rock limits isotope exchange: Given that the isotope exchange capacity of the fluid is low, the mineral with the second highest diffusivity of the respective isotope will govern the effective closure of all minerals of an assemblage, as pointed out by Giletti (1991) and Ehlers and Powell (1994). As far as eclogites are concerned, literature data indicate that the temperature required for activation of significant Sr diffusion are as follows in increasing order: 600–650°C for white mica (cf. Villa, 1998) near 650°C for apatite (Cherniak and Ryerson, 1993) 625–700°C for amphibole (Brabander and Giletti, 1995), and very high temperatures of 800–1000°C for clinopyroxene

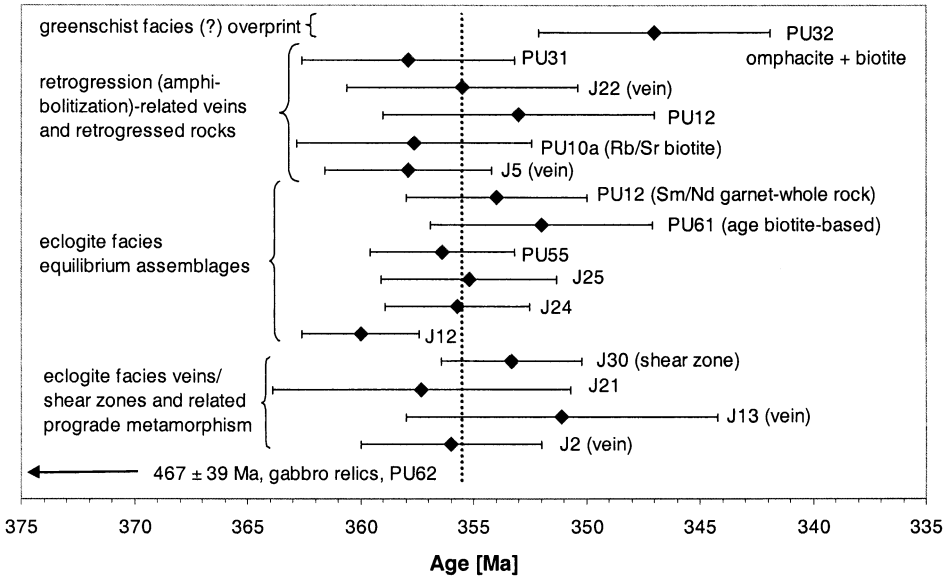

Fig. 5. Compilation of age data for Marun-Keu rocks. Vertical stippled line: Average age of both eclogite and amphibolite facies assemblages (355.5 ± 1.4 Ma, Tukey's Biweight Mean).

Table 4. XRF whole rock analyses for major- (wt-%) and trace- (ppm) elements.

	PU31a	PU31c	PU31d	J12 a	J12 b	J12 c	J30	J32a	J32c	PU 4c
	amphib.	trans.	eclogite	eclogite	trans.	gar-amp	shear z.	eclogite	trans.	vein
SiO_2	52.4	52.3	50.3	52.95	53.35	47.12	71.77	53.29	49.55	39.60
TiO_2	1.11	1.15	1.19	0.62	0.33	0.42	0.46	0.89	0.94	0.12
Al_2O_3	13.90	14.40	14.80	17.87	16.19	16.67	13.14	15.16	16.43	32.14
Fe_2O_3	11.38	11.78	12.27	3.51	7.6	9.06	3.76	8.74	9.69	3.67
MnO	0.18	0.18	0.19	0.02	0.12	0.15	0.06	0.16	0.17	0.10
MgO	6.4	6.65	6.98	6.67	7.87	13.17	1.39	6.15	7.13	4.87
CaO	10.08	10.69	10.90	8.90	8.54	7.67	5.02	8.77	9.04	3.08
Na_2O	2.03	1.71	2.30	4.56	3.63	3.45	0.54	3.39	3.45	4.90
K_2O	0.44	0.45	0.49	3.01	1.56	1.00	2.01	1.94	2.02	1.59
P_2O_5	0.16	0.17	0.15	0.14	0.02	0.06	0.17	0.15	0.05	0.00
BaO	—	—	—	0.08	0.03	0.02	0.05	0.05	0.06	0.15
H_2O	1.46	0.79	0.64	—	—	—	—	—	—	—
CO_2	0.123	0.099	0.123	—	—	—	—	—	—	—
LOI	—	—	—	1.59	0.66	1.15	1.06	0.77	0.93	2.25
Sum	99.68	100.41	100.36	99.83	99.86	99.90	99.39	99.40	99.40	92.31
Density	3.11	3.18	3.35	—	—	—	2.86	3.20	—	—
V	264	242	295	148	93	87	25	208	277	125
Cr	395	383	479	253	722	793	84	562	565	79700
Co	41	46	44	17	33	65	8	25	38	29
Ni	68	75	76	104	174	379	17	64	113	448
Cu	24	21	19	24	13	9	11	58	75	12
Zn	92	96	96	53	59	138	15	67	87	137
Th	<2	<2	<2	19	<2	<2	13	5	3	<2
U	<2	4	3	4	2	>2	4	<2	3	<2
Y	33	32	32	8	15	13	41	31	29	<1
Zr	98	98	100	267	49	47	388	118	120	<5
Nb	3	5	3	6	1	3	8	10	7	6
Pb	6	5	7	9	8	7	18	7	<5	40
Rb	20	20	21	143	72	36	56	58	60	34
Sr	183	217	180	407	216	161	437	56	75	9470

Major and trace elements analysed by XRF on fused glass discs and powder pellets at Oslo University and at GFZ Potsdam. Loss on ignition (LOI) was determined gravimetrically after igniting the sample powder to 1050°C for 1 h. amphib.: amphibolite; trans.: transition; gar-amp: garnet amphibolite; shear z.: shear zone.

(Sneeringer et al., 1984; Cherniak, 1998) and garnet (cf. Coghlan, 1990). Therefore even in presence of fluids no significant Sr isotope exchange among minerals occurs, if temperatures are below the "closure temperatures" for apatite and amphibole, i.e., below 650 to 700°C. The estimates for maximum eclogite facies temperatures in the Marun-Keu complex are close to 650°C (Molina et al., 2002). Given that fluid-present eclogite facies conditions did not last for very long time, postcrystallization intermineral Sr isotope exchange consequently was largely insignificant even in presence of fluids, and preservation of equilibration/crystallization ages in the Rb/Sr systematics is likely. The absence of grain size—age correlations in the phengite populations (e.g., samples J30/J32; J12; Fig. 4) and the fact that for some samples high-Sr-retentivity systems like omphacite-whole rock co-define the ages (e.g., J12, Fig. 4) similarly indicate that crystallization-

Table 5. Fission track data, Marun-Keu complex.

Sample	Irr. No.	No. of ctd. grains	$\rho d \times 10^4$ cm^{-2} (counted)	$\rho s \times 10^4$ cm^{-2} (counted)	$\rho i \times 10^4$ cm^{-2} (counted)	$P(\chi^2)$ % (var%)	Mean track length (μm)	Standard deviation (μm)	Central age $\pm 2\sigma$ (Ma)
J12a ap	116–3	17	161 (4417)	110 (566)	122 (628)	50 (7)	13.64 ± 0.20	1.44 (54)	252 ± 32
Pu12 ap	116–7	13	148 (4417)	209 (565)	219 (592)	99 (0)	12.44 ± 0.22	1.74 (64)	246 ± 30
Pu22 ap	116–8	19	145 (4417)	33.0 (354)	34.9 (375)	99 (0)	nd	nd	238 ± 36
J30 zir	121–31	7	38.3 (2747)	1276 (516)	126 (51)	97 (0)			228 ± 67
J12a zir	121–29	4	41.86 (2747)	3049 (525)	290 (50)	90 (0)			259 ± 76
J3 zir	121–30	12	38.89 (2747)	1141 (1256)	95.4 (105)	88 (0)			273 ± 56

ap, apatite; zir, zircon. ρs and ρi represent sample spontaneous and induced track densities; ρd represents standard track density. $P(\chi^2)$ is the probability of χ^2 for v degrees of freedom where v = no. of crystals − 1. nd, not determined. All ages are central ages (Galbraith, 1981). $\lambda_D = 1.55125 \times 10^{-10}$. A geometry factor of 0.5 was used. Zeta = 360 ± 5 for CN5/apatite and 120 ± 8 for CN1/ zircon. Irradiations were performed at the ANSTO facility, Lucas Heights, Australia.

related isotope systematics are preserved (cf. Glodny et al., 2002).

In fluid-absent (dry) rocks, an effective mass transfer mechanism along grain boundaries does not exist. Diffusion along anhydrous grain boundaries is extremely slow (Rubie, 1986), and the width of dry grain boundaries between silicate grains does not exceed a few atom diameters (e.g., Veblen and Buseck, 1981), implying that the relative volume of grain boundaries in a rock is very small. Consequently, the impact of grain boundary diffusion on the overall scale of mass transport is minimal (Joesten, 1991). Therefore, in fluid-absent rocks isotope exchange is governed by closed-system cation interdiffusion dynamics which follows complex rules, completely different from those forming the base of Dodson's (1973) theory of cooling ages. In such a situation, diffusion takes place as *local two-phase cation (and isotope) interdiffusion*, between mineral grains connected by grain boundaries, as modeled e.g., by Ehlers and Powell (1994). Any isotope exchange will occur only if two adjacent grains are simultaneously "open" for diffusion *and* have significant intrinsic concentrations of the diffusing species. If a mineral (e.g., phengite) is surrounded either by Sr-free minerals (e.g., quartz) or by minerals with very sluggish Sr diffusion (omphacite, garnet) it will remain as a closed system irrespective of internal Sr mobility, and isotopic signatures are preserved unless temperatures are high enough to activate Sr diffusion in neighbouring phases. In fluid-absent eclogites, *matrix-dependent, modally controlled closed system behaviour* is expected. In the analyzed Marun-Keu eclogites, phengite, amphibole and apatite, i.e., those minerals in which diffusion may be activated at the metamorphic temperatures reached, are usually accessory minerals, while omphacite, garnet and quartz dominate the rock mode. Abundant direct contacts between the high-diffusivity phases are statistically improbable. Therefore, in the same way as fluid-absent eclogites preserve the very P,T conditions of fluid-aided crystallization (Engvik et al., 2000), they should record crystallization ages in their Rb/Sr-systematics.

The potential of matrix-dependent, modally controlled closed system behaviour in preserving isotopic signatures is tremendous: Kelley and Wartho (2000) showed that phlogopite grains in mantle xenoliths from kimberlites preserved Ar-Ar ages recorded at mantle ambient temperatures, 700°C above the "conventional" closure temperature.

The above discussion shows that intermineral Sr isotope exchange in eclogites was negligible given the rock remained devoid of free fluids. Fluid absence is indicated for many eclogites of this study *after eclogite facies conditions* by complete absence of retrogression phenomena. Had any free aqueous fluid been present after the end of eclogite facies conditions, its catalytic effect would have erased HP phases and converted the eclogites into amphibolite- or greenschist facies rocks (cf. Rubie, 1986, 1990; Carswell et al., 2000).

However, fluid may have been present for some time after eclogitization but still at eclogite facies conditions, possibly enabling some postcrystallizational Sr isotope exchange. If in such a period *prolonged* exchange of Sr between mica (with its *t*-dependent increasingly radiogenic Sr) and other phases had occurred, the radiogenic Sr must be present in adjacent phases. It can clearly be anticipated that in such a situation, in a rock containing phases with different grain sizes and different Sr diffusivities, continuous and complete Sr-isotopic equilibration is impossible, and radiogenic Sr will be irregularly distributed. A rough calculation shows that statistically valid multimineral isochrons will not be obtained, unless the period of Sr isotope exchange was very short, i.e., on the order of the error of the age determination. In other words: *Valid multimineral isochron ages cannot be interpreted as cooling ages*. Therefore, our observation of valid isochrons proves absence of significant postcrystallizational Sr isotope exchange, and suggests fairly rapid "drying out" of the eclogites after reaction. Very short timescales for eclogite facies reactions and vein formation, on the order of <1 Ma, have similarly been suggested by Widmer and Thompson (2001). We conclude that the age data for eclogites and eclogite facies veins represent crystallization ages. Field evidence shows that introduction of fluids causes eclogitization, and consequently, the Rb/Sr ages reflect *eclogitization.* They date fluid-induced metamorphic reactions rather than peak-metamorphic conditions or cooling.

For the retrogression-related veins and the amphibolitized rocks, several lines of evidence suggest that the age data represent crystallization ages as well: First, statistically valid multimineral isochrons were obtained. Second, the hydration reactions around amphibolite facies veins are not kinetically inhibited (Yardley, 1997) and therefore possibly rapid. Reaction stops when the fluid is consumed by the hydration reactions. Overall fluid deficiency at amphibolite facies conditions is obvious from the abundant preservation of eclogite. Therefore, immediately after the amphibolitization reactions the rock was devoid of free fluids, which again implies preservation of crystallization-related isotope signatures. Third, most amphibolite facies assemblages are composed only of minerals which either are trace phases (biotite) or have low Sr diffusivities (amphibole, phengite and garnet as cited above; significant Sr diffusion in feldspar is activated only at temperatures in excess of $\sim$600°C, cf. Cherniak, 1996), implying likely *preservation of crystallization-related isotopic signatures* in most minerals.

Protolith relics. Largely preserved gabbroic relic assemblages (sample PU62, Fig. 2a) concur with a preserved protolith Rb/Sr isotope distribution. Despite the metamorphic temperatures of ca 650°C, the Rb/Sr isochron age of 467 $\pm$ 39 Ma (Fig. 4) is, within limits of error, identical to the age of protolith crystallization (zircon Pb evaporation data, Glodny et al., 1999). It has been shown before that mafic protolith relics to eclogite facies metamorphism may preserve their Rb/Sr systematics through metamorphic temperatures of even $>$730°C (Miller and Thöni, 1995). Together, these data illustrate the persistence of crystallization-related Sr isotope distributions in petrographic relics through very high temperatures given that fluid-absent conditions prevail.

6.2. Sm/Nd Data for Marun-Keu Eclogites

The Sm/Nd data for garnet and whole rock of sample PU12 (Table 3) define a two-point isochron, corresponding to an age of 354 $\pm$ 4 Ma. The garnet was formed during eclogitization of the rock. Therefore the age confirms the Rb/Sr age data for eclogite facies metamorphism. However, other samples had either virtually no spread in Sm/Nd ratios between minerals for unknown reasons, or Nd-isotopic disequilibria (e.g., sample PU22, Table 3). The disequilibria may represent isotope distri-

butions inherited from the protoliths (e.g., Thöni and Jagoutz, 1992).

6.3. Eclogite Facies Fluids

The involvement of fluids in eclogitization and eclogite facies processes in the Marun-Keu complex is evident from the fluid-related partial eclogitization of protoliths, from the formation of eclogite facies veins, and the occurrence of eclogite facies reaction haloes around fluid pathways (Figs. 2a, 2b, 3). Similar observations were made in other eclogite complexes, and confirmed experimentally (Holland, 1979; Laird and Albee, 1981; Selverstone et al., 1992). Presence of fluids at eclogite facies conditions seems to be essential to overcome kinetic barriers for eclogitization, as suggested by field evidence (e.g., Rubie, 1990; Austrheim, 1998 our sample PU62). Ongoing discussion centers around the origin of the fluids, their physicochemical properties and the amount of fluids at depth.

Several samples of this study record perfect initial Sr-isotopic equilibrium between eclogite facies veins and their immediate wallrocks. Among these samples (cf. Table 2 and Appendix) are J2 (quartzitic vein in foliated eclogite), J30/J32 (fluid pathway with eclogite facies reaction aureola) and J12 (transition: eclogite–garnet amphibolite). In contrast, significant differences of initial Sr isotopic compositions exist between different eclogite facies veins (Sr_i between 0.705440 $\pm$ 0.000047 for sample J21 and 0.709174 $\pm$ 0.000054 for sample J13, see Table 2), indicating that there was no single large fluid reservoir and no interconnected network of fluid reservoirs with rapid internal equilibration.

We interpret this as being indicative for *local* physicochemical equilibrium between fluids and host rock. The fluids must either be advected but readily equilibrated with the surrounding rocks, or they must be locally derived, e.g., by decrepitation of fluid inclusions (Philippot and Selverstone, 1991) or by fluid-releasing mineral reactions (Gao and Klemd 2001). We favour a local derivation or at least long-term immobility of the fluids because rapid equilibration between advected, probably solute-rich (cf. Philippot and Selverstone, 1991; Scambelluri and Philippot, 2001) high-pressure fluids and the wallrock of the veins is unlikely: the high metasomatic capacity of isotopically exotic fluids would imply Sr-isotopic gradients on the mineral and hand specimen scale (as shown by Franz et al., 2001 for Pb isotopes), as well as Sr metasomatism in the wallrocks of veins, which is not observed in the here presented dataset. The data do not allow to trace the fluids to sources different from the local rocks, but favour restricted fluid flow, Sr-isotopically different sources for the fluids, short-range fluid migration, and effective fluid compositional buffering by the local host rocks. This interpretation is supported by the petrographic observation that most veins are not interconnected and of variable mineralogical composition.

Local equilibrium between high-pressure fluids and surrounding rocks, whether by internal buffering or due to local fluid derivation, seems to be a general phenomenon. Such equilibria were similarly found elsewhere, with different approaches including compositional correlation between vein- and rock-forming clinopyroxenes (Scambelluri et al., 1998), petrology and fluid inclusion studies (Selverstone et al., 1992), radiogenic isotopes (Becker et al., 1999), C-H-O isotope data (Nadeau et al., 1993) and combination of fluid inclusion with stable isotope data (Gao and Klemd, 2001). For the Marun-Keu, local fluid-rock equilibria are inferred from O isotope data as well (M. Leech, private communication). Together, the available stable and radiogenic isotope data point to local (cm— to m-scale) equilibrium between rocks and fluids in the studied rocks. The results argue against models which suggest large scale fluid flow of isotopically homogeneous fluids during HP metamorphism (e.g., Bebout, 1991 and references therein).

However, it needs to be stressed that this conclusion of restricted fluid flow cannot be generalized. Phenomena like arc magmatism and serpentinization of suprasubduction zone mantle wedges imply that pathways for fluid escape from eclogitization zones must exist, at least locally. In fact, current work in the Marun-Keu complex by J. F. Molina et al. unveiled a vein system with significant fluid transfer, indicating that at depth large domains with static fluids coexist with local zones of long-range fluid transport.

The fluid-rock ratio during eclogitization was probably low. Reactions can start and proceed even in the presence of only a small quantity of free fluid (<1%), which acts as a catalyst (Hacker, 1996). The maximum amount of fluid can be estimated from the abundance of quartzitic veins: Given that less than 0.1% of the rock consists of veins, and that fluids in equilibrium with quartz at 600°C and 1.5 GPa contain $\sim$ 2–3 wt.% SiO_2 in solution (Manning, 1998), a fluid/rock mass ratio of <0.03 calculates if all SiO_2 is precipitated. This is a maximum estimate since other studies point to much higher silicate solubilities in high pressure fluids (cf. Scambelluri and Philippot, 2001). The overall fluid deficiency in the complex, evident from incomplete eclogitization, similarly points to only small amounts of fluids. Metasomatic effects of the fluids are present but of minor importance; in some transition samples (e.g., samples J32a vs. J32c, Table 4), reactions were nearly isochemical with respect to most elements. Most of the veins therefore may be interpreted, in line with the interpretation of the isotope data, as local segregation phenomena (e.g., Widmer and Thompson, 2001), which do not require large amounts of fluids.

6.4. Retrogressive Fluids

After eclogitization, the amount of free fluid in the rock is expected to be small since fluids are consumed in the metamorphic reactions, and most excess free fluids will be expelled at high grade conditions. During early cooling and/or decompression, incipient retrograde reactions produce hydrated minerals thus consuming water. Therefore shortly after peak metamorphism the HP rocks should lack free fluids (Yardley, 1997). This fluid absence kinetically inhibits retrograde rock conversion. Re-entrance of fluids is necessary to overcome the kinetic barrier and is possible by essentially two mechanisms, namely infiltration from extraneous sources, and in-situ generation of fluid by retrograde reactions. For fluid infiltration, pathways have to be created by tectonic fracturing during exhumation, or by hydraulic fracturing (e.g., Barnicoat, 1988). Small amounts of fluids can be generated in situ, during decompression, in some eclogite facies lithologies by the (autocatalytic) reaction

paragonite + white mica I (high phengite)+ garnet $\Leftrightarrow$ white mica II (low phengite) + biotite + plagioclase + quartz + H_2O

(Heinrich, 1982). Dependent on the mode of the eclogite facies rock, the fluids produced this way may be internally consumed by hydration reactions or may leave the rock and cause retrogression reactions elsewhere. The above reaction is most likely to occur in felsic lithologies, in particular in metapelites (Heinrich, 1982). While in some former felsic eclogite facies rocks of the Marun-Keu complex this reaction may have occurred, in most mafic eclogites of the complex it did not take place due to lack of reactants. The local retrogression of these lithologies was due to fluid infiltration, from other lithologies or from outside the complex, as evident from the amphibolite facies veining (Figs. 2c, 2d). Large volumes of rock lack evidence for retrogression reactions, indicating that there was a general fluid deficiency during exhumation.

It is an open question where the retrogressive fluids in the Marun-Keu complex came from. Large scale fluid influx from outside may leave a metasomatic imprint that may also be detectable in Sr isotope systematics. However, our Sr isotope data, e.g., the isotopic record from sample PU31 (Table 2) shows that the retrogressive fluids were in local Sr-isotopic equilibrium with the rock as the amphibolitization apparently did neither change the Sr isotopic composition of the whole rock system nor element concentrations (analyses No. PU31a,c,d in Table 4). Furthermore, retrograde breakdown of omphacite and recrystallization of white mica and apatite during amphibolitization (see Rb, Sr concentration data for the two latter phases, Table 2) indicates that all major Sr-bearing phases were open for Sr exchange with the fluid during the retrogression reactions, i.e., that the rocks had a high buffering capacity. Apparently the Rb/Sr system of the fluids was buffered by the local rock composition thus implying addition to the rock of only small amounts of fluids, the source of which cannot be clearly constrained. The fluids were readily equilibrated with the local rock and finally consumed by hydration reactions.

6.5. Eclogite Facies Fluid-Rock Equilibria

Field evidence suggests that not all amphibole-dominated assemblages in the Marun-Keu are products of retrograde metamorphism. In particular, samples J 12 and J30/J32 (Figs. 2b, 3) present transitions between garnet amphibolite and omphacite-rich eclogite which are most probably not retrograde transitions but rather reflect fluid-driven eclogitization. One possible interpretation is that these transitions represent fluid-induced prograde reactions, and that the garnet amphibolites form the protolith of the eclogites. However, in this case the amphibole-dominated assemblages must have been formed immediately, less than a few Ma before the eclogite-forming event because otherwise the amphibole-dominated lithologies would yield older ages than the eclogite, which is not observed. An alternative interpretation is contemporaneous formation of the eclogitic and the garnet amphibolite assemblages, at the same P and T, as suggested by Molina et al. (2002) e.g., for sample J12a-c. Different assemblages would then reflect local differences in fluid availability, fluid composition and in the fluid's solutes budget. Reaction textures, like mineral zoning, may be caused by short-term shifts in the fluid properties. This interpretation is favoured by the (at first hand surprising) observation of perfect initial Sr-isotopic equilibria across these transitions (Table 2). The isotopic equilibria are most easily explained by crystallization of all phases in the presence of one continuous fluid film. The possibility that rocks of similar bulk composition (e.g., J32a, J32c, Table 4), dependent on the fluid budget, develop different assemblages has already been proposed e.g., by Yoder (1952), Brown and Bradshaw (1979), Maresch and Abraham (1981), and Heinrich (1982). Development of different assemblages during identical P,T conditions is even more likely for samples with pronounced gradients in bulk rock chemical composition (e.g., J12a-c, Table 4).

6.6. Fluids, and Eclogite Facies Deformation

Eclogite facies ductile deformation is focused or even restricted to zones containing free fluids. Strain is in most cases partitioned into rocks adjacent to fluid veins (sheared eclogite of sample J12, Fig. 2b) or into fluid-bearing shear zones (samples J30/J32, Fig. 3). The correlation between fluids, deformation and metamorphic reaction kinetics can be explained as a feedback interdependency of these factors: Deformation is facilitated and favored by fluid-mediated rapid mass transfer (cf. Nakashima, 1995). Deformation in turn enhances hydraulic conductivity, which promotes further weakening in the shear zone and further reaction progress in formerly metastable rocks (cf. Austrheim, 1998). Strong partitioning of strain into (fluid-bearing) shear zones is similarly observed in many other HP complexes (Jamtveit et al., 1990; Markl and Bucher, 1997; Tilton et al., 1997). Fluid-absent lithologies may escape from both metamorphic transformation and deformation, which enables preservation of premetamorphic textures (Austrheim et al., 1997). In the Marun-Keu complex, lithologies are present which show fluid-mediated eclogitization but escaped from penetrative deformation (e.g., the central, eclogitic part of sample J 12, Fig. 2b). This suggests that either a certain fluid-rock ratio or a prolonged presence of fluids is necessary for to start deformation. Several quartzitic veins as well as some foliated eclogites experienced static recrystallization, indicating that deformation ceased before the rocks finally dried out. Perfect preservation of eclogitic assemblages implies that both drying out, and termination of ductile shearing occurred at still eclogite facies conditions.

6.7. Veining in the Rai-Iz Ophiolites: Implications for the Polar Urals Paleosubduction Zone

The Rb/Sr data of the metasomatic veins in the Rai-Iz ophiolite complex yield an isochron age of 373.1 $\pm$ 5.4 Ma (Table 2, Fig. 4), which we interpret as an undisturbed crystallization age. Several observations point to subduction fluids as the mineralizing agent. The Si, Al, Na, K-dominated elemental chemistry of the veins (PU4, Table 4) is indicative for fluids originally liberated at depths of $\sim$50 km, during subduction-related prograde metamorphism of mafic lithologies (Manning, 1998; Gao and Klemd, 2001). A suprasubduction zone mantle wedge setting for the Rai-Iz complex, with influx of subduction fluids, was independently suggested by Garuti et al. (1999), based on a study of platinum-group element mineralogy of the complex. The initial εNd-value of the vein material is +3 (Table 3), in contrast to a value of +8.6 $\pm$ 1.8 in the matrix rocks (Sharma et al., 1995). The initial $^{87}Sr/^{86}Sr$ ratio of the vein (0.70482 $\pm$ 0.00002, Table 2) contrasts with the lower

values expected and extrapolated for the unaltered wallrock (cf. Sharma et al., 1995). Together, the geochemical and isotopic evidence suggest fluid derivation from subducted, dehydrating, probably oceanic, crustal material.

Our preferred geodynamic interpretation is that the Polar Urals paleosubduction system was active already at ~373 Ma, i.e., ~18 Ma before eclogitization of the Marun-Keu complex (~355 Ma). E-directed subduction of oceanic crust at early stages was followed by subduction of the thinned East European margin and, finally, of continental crust, represented by todays Marun-Keu complex. Subduction of Marun-Keu-like continental crust will block up the subduction zone, as inferred from buoyancy analysis (e.g., Cloos, 1993). This blocking-up event at ~355 Ma marks onset of continent-island arc collision tectonics, with concomitant exhumation of the Marun-Keu complex.

6.8. Exhumation Rate

Combining the metamorphic conditions for eclogitization (14–17 kbar, 520°–690°C) and later amphibolitization (8–12 kbar, 535°-575°C for sample PU31) with the respective age data suggests an early stage of rapid decompression. Using the age data for sample PU31 (eclogitization and amphibolitization indistinguishably at 357.9 ± 4.7 Ma, i.e., within a time frame of <9.4 Ma), the metamorphic pressure difference of 5.5 ± 3.5 kbar, and a rock density of 2.9 g/cm^3 leads to an average exhumation rate of 2 ± 1.3 km/Ma. This result most probably underestimates the true exhumation rate as the other age data suggest an even narrower time frame between eclogitization and amphibolitization. The rate estimate is, however, independent from problematic assumptions on closure temperatures and isotope diffusion parameters.

6.9. Postmetamorphic Thermal History

As outlined above, the Rb/Sr isotope data date fluid-rock-interaction rather than cooling, and cannot be used to constrain cooling rates in the high temperature regime. The upper crustal cooling and exhumation history is inferred from zircon and apatite fission track (FT) data. Both zircon and apatite FT ages cluster around 250 Ma (Table 5). The zircon FT closure temperature is estimated at ~300°C (cf. Dahl, 1997; Stöckhert et al., 1999) which indicates a midcrustal position, at T >300°C, for the Marun-Keu until the Triassic. It is worth noting that the biotite Rb/Sr data, e.g., for sample PU10a (Table 2) do not reflect the Triassic cooling. Instead, crystallization ages are preserved. The apatite FT closure temperature is approximately 110° ± 10°C, with partial annealing down to 60°C (Green et al., 1989). The coincidence within limits of error of the zircon and apatite FT ages point to a distinct event of 'rapid' exhumation at ~250 Ma, in accordance with independent evidence for compression, and erosion of metamorphic complexes in the Polar Urals in Triassic time (cf. Bogdanov et al., 1996; Sobornov and Rostovshchikov, 1996; Mørk, 1999). Furthermore, the fission track ages are similar to those obtained for and near the Maksyutov eclogite complex, Southern Urals (Leech and Stockli, 2000; Seward et al., 2002). This suggests a comparable Early Mesozoic exhumation history for HP complexes all along the western flank of the Uralides.

7. CONCLUSIONS

Rb/Sr internal mineral-isochron ages constrain the fluid-rock interaction history of the Marun-Keu complex, during both late prograde and early retrograde metamorphic stages. The isotopic record is generally preserved when the rocks were devoid of free fluids; fluid-rock interaction caused isotopic resetting. Magmatic protoliths are locally preserved, due to fluid-absent conditions throughout the metamorphic history. Their Rb/Sr mineral systematics reflect magmatic crystallization despite of later metamorphic temperatures of ~650°C. The Rb/Sr mineral data *provide hygrochronological rather than thermochronological constraints*.

For fluid-absent rocks, with the possible exception to ultrahigh temperature rocks like granulites, the classical theory of cooling ages does not apply. Instead, *matrix-dependent, modally controlled closed system behaviour* controls isotope distributions. This enables to employ Rb/Sr (and possibly U/Pb, Sm/Nd.. . .) internal mineral isochrons for establishing detailed petrologic histories for metamorphic rocks, provided that during reaction, isotopic equilibrium was achieved and that, after crystallization, the rocks remained devoid of free fluids. "Dryness" of a rock outside its thermodynamic stability field implies its metastable preservation as a petrographic relic, and is easy to recognize by absence of retrogression-related petrographic (and isotopic) disequilibria.

Vein assemblages are particularly useful for deciphering of metamorphic reaction histories as they are direct evidence for fluid presence. From the veins and their immediate wallrock, possibly both crystallization P,T conditions and the exact age of crystallization can be derived, thus providing a well-constrained anchorpoint for P,T,t path reconstructions. Sr isotope systematics for the studied eclogite facies veins and their wallrocks point to restricted fluid flow, absence of a large interconnected fluid reservoir network, and to local, Sr-isotopically different sources for the fluids. The retrograde, amphibolite facies vein assemblages similarly show initial Sr-isotopic equilibrium with their immediate, retrogressed wallrocks, suggesting a high buffering capacity of the reacting wallrocks, and influx of only minor amounts of fluids which were readily consumed by hydration reactions.

In the Marun-Keu complex, prograde eclogitization was closely followed by retrograde amphibolitization. Ages for prograde and retrograde assemblages overlap in time within limits of error at 355.5 ± 1.4 Ma. Early exhumation rates exceeded 2 ± 1.3 km/Ma. With this rapid metamorphic and geodynamic evolution, the Marun-Keu contrasts with some other HP complexes that show prolonged HP histories: In the Sesia-Lanzo Zone, eclogite facies conditions prevailed for >16 Ma (Inger et al., 1996). De Sigoyer et al. (2000) documented a time span of ~8 Ma between eclogitization and retrogressive amphibolitization in Himalayan eclogites. In the Bergen arcs, Norway, this age difference amounts to ~10–15 Ma (Glodny et al., unpublished data).

Subduction fluids not only play a major role in reaction kinetics and isotopic equilibration during metamorphism but can be traced into the suprasubduction zone mantle wedge. For the Polar Urals paleosubduction system, fluids caused metasomatic vein formation in mantle rocks at 373.1 ± 5.4 Ma, already ~18 Ma before the subduction zone was jammed by

introduction of the leading edge of the East European continent, which forms todays Marun-Keu complex.

Acknowledgments—Parts of this work were funded by a grant of the European Commission (TMR-URO Programme, research network contract No. FMRX-CT96-0009 (DG 12-ORGS)). Financial support by the Research Council of Norway (NFR) and by the Nansen Foundation is gratefully acknowledged, as well as field trip organization by D. G. Gee and his team. We are indebted to V. Dushin, V. Koroteev, E. Khain, G. Savelieva and particularly V. Lennykh for excellent expert guidance in the field area. K. Mezger is thanked for his permission to carry out some Rb/Sr analyses at the Zentrallaboratorium für Geochronologie, Universität Münster. The various efforts (figure design, sample processing, photography) of G. Bye Fjeld, J. Herwig, D. Woroschuk, J. Løkken, M. Langanke, T. Enger, R. Naumann, M. Dziggel and B. Stöcker are gratefully acknowledged. The manuscript benefited from discussions with R. Hetzel, K. Gräfe and R. L. Romer. We thank B. Bingen, R. Klemd, B. R. Frost (AE) and an anonymous reviewer for their careful and constructive reviews. This is an Europrobe publication.

Note: Vladimir Lennykh deceased on January 2, 2002. He was an enthusiastic geologist, and we will not forget the "good company" during fieldwork. We dedicate this work to his memory.

Associate editor: B. Ronald Frost

REFERENCES

Ahrens T. J. and Schubert G. (1975) Gabbro-eclogite reaction rates and its geophysical significance. *Rev. Geophys. Space Phys.* **13,** 383–399.

Austrheim H., Erambert M., and Engvik A. K. (1997) Processing of crust in the root of the Caledonian continental collision zone: The role of eclogitization. *Tectonophysics* **273,** 129–153.

Austrheim H. (1998) Influence of Fluid and Deformation on Metamorphism of the Deep Crust and Consequences for the Geodynamics of Collision Zones. In *When continents collide: Geodynamics and geochemistry of Ultrahigh-Pressure Rocks* (eds. B. R. Hacker and J. G. Liou), pp. 297–323. Kluwer, Dordrecht.

Barnicoat A. C. (1988) The mechanism of veining and retrograde alteration of Alpine eclogites. *J. Metamorph. Geol.* **6,** 545–558.

Bebout G. E. (1991) Field-based evidence for devolatilization in subduction zones: implications for arc magmatism. *Science* **251,** 413–416.

Becker H., Jochum K. P., and Carlson R. W. (1999) Constraints from high-pressure veins in eclogites on the composition of hydrous fluids in subduction zones. *Chem. Geol.* **160(*4*),** 291–308.

Biino G. G. and Compagnoni R. (1992) Very-high pressure metamorphism of the Brossasco coronite metagranite, southern Dora Maira massif, Western Alps. *Schweiz. Mineral. Petrogr. Mitt.* **72,** 347–363.

Blanckenburg F. v., Villa I. M., Baur H., Morteani G., and Steiger R. H. (1989) Time calibration of a PT-path from the Western Tauern Window, Eastern Alps: the problem of closure temperatures. *Contrib. Mineral. Petrol.* **101,** 1–11.

Bogdanov N. A., Khain V. E., Bogatsky V. I., Kostyuchenko S. L., Senin B. V., Shipilov E. V., and Sobolev S. F. (1996) Tectonic map of the Barents Sea and the Northern part of European Russia, with Explanatory Notes. Institute of the Lithosphere, RAS, Moscow.

Brabander D. J. and Giletti B. (1995) Strontium diffusion kinetics in amphiboles and significance to thermal history determinations. *Geochim. Cosmochim. Acta* **59,** 2223–2238.

Brown E. H. and Bradshaw J. Y. (1979) Phase relations of pyroxene and amphibole in greenstone, blueschist and eclogite in the Franciscan Complex, California. *Contrib. Mineral. Petrol.* **71,** 67–83.

Carswell D. A. (1990) Eclogites and the eclogite facies; definitions and classification. In *Eclogite facies rocks* (ed. D. A. Carswell) pp. 1–13. Blackie, Glasgow.

Carswell D. A., Wilson R. N., and Zhai M. (2000) Metamorphic evolution, mineral chemistry and thermobarometry of schists and orthogneisses hosting ultra-high pressure eclogites in the Dabieshan of central China. *Lithos.* **52,** 121–155.

Cherniak D. J. (1996) Strontium diffusion in sanidine and albite, and general comments on strontium diffusion in alkali feldspars. *Geochim. Cosmochim. Acta* **60,** 5037–5043.

Cherniak D. J. (1998) Pb diffusion in clinopyroxene. *Chem. Geol.* **150,** 105–117.

Cherniak D. J. and Ryerson F. J. (1993) A study of strontium diffusion in apatite using Rutherford backscattering spectroscopy and ion implantation. *Geochim. Cosmochim. Acta* **57,** 4653–4662.

Cliff R. A., Barnicoat A. C., and Inger S. (1998) Early Tertiary eclogite facies metamorphism in the Monviso Ophiolite. *J. Metamorph. Geol.* **16,** 447–455.

Cloos M. (1993) Lithospheric buoyancy and collisional orogenesis: subduction of oceanic plateaus, continental margins, island arcs, spreading ridges, and seamounts. *Geol. Soc. Am. Bull.* **105,** 715–737.

Coleman R. G., Lee D. E., Beatty L. B., and Brannock B. B. (1965) Eclogites and eclogites: their differences and similarities. *Geol. Soc. Am. Bull.* **76,** 483–508.

Coghlan R. A. N. (1990) Studies in diffusional transport: grain boundary transport of oxygen in feldspars, diffusion of oxygen, strontium, and REEs in garnet, and thermal histories of granitic intrusions in South-Central Maine using oxygen isotopes. Ph. D. thesis, Brown Univ., Providence R.I.

Dahl P. S. (1997) A crystal-chemical basis for Pb retention and fission-track annealing systematics in U-bearing minerals, with implications for geochronology. *Earth Planet. Sci. Lett.* **150,** 277–290.

De Sigoyer J., Chavagnac V., Blichert-Toft J., Villa I. M., Luais B., Guillot S., Cosca M., and Mascle G. (2000) Dating the Indian continental subduction and collisional thickening in the Northwest Himalaya; multichronology of the Tso Morari eclogites. *Geology* **28***(6)* 487–490.

Dobretsov N. L. and Sobolev N. V. (1984) Glaucophane schists and eclogites in the folded systems of northern Asia. *Ofioliti* **9,** 401–424.

Dodson M. H. (1973) Closure temperature in cooling geochronological and petrological systems. *Contrib. Mineral. Petrol.* **40,** 259–274.

Dodson M. H. (1979) Theory of cooling ages. In *Lectures in isotope geology* (eds. E. Jaeger and J. C. Hunziker), 194–202. Springer, Berlin.

Ehlers K. and Powell R. (1994) An empirical modification of Dodson's equation for closure temperature in binary systems. *Geochim. Cosmochim. Acta* **58,** 241–248.

Engvik A. K., Austrheim H., and Andersen T. B. (2000) Structural, mineralogical and petrophysical effects on deep crustal rocks of fluid-limited polymetamorphism, Western Gneiss region, Norway. *J. Geol. Soc. London.* **157(1)** 121–134.

Ernst W. G., Mosenfelder J. L., Leech M. L., and Liu J. (1998) H_2O recycling during continental collision: phase-equilibrium and kinetic constraints. In *When continents collide: Geodynamics and geochemistry of Ultrahigh-Pressure Rocks* (eds. B. R. Hacker and J. G. Liou), pp. 275–295. Kluwer, Dordrecht.

Farquhar J., Chacko T., and Ellis D. J. (1996) Preservation of oxygen isotope compositions in granulites from Northwestern Canada and Enderby Land, Antarctica: implications for high-temperature isotopic thermometry. *Contrib. Mineral. Petrol.* **125,** 213–224.

Franz L., Romer R. L., Klemd R., Schmid R., Oberhänsli R., Wagner T., and Shuwen D. (2001) Eclogite-facies quartz veins within metabasites of the Dabie Shan (eastern China); pressure-temperature-time-deformation path, composition of the fluid phase and fluid flow during exhumation of high-pressure rocks. *Contrib. Mineral. Petrol.* **141,** 322–346.

Galbraith R. F. (1981) On statistical models for fission track counts. *J. Intnl. Assoc. Math. Geol.* **13, 6,** 471–478.

Gao J. and Klemd R. (2001) Primary fluids entrapped at blueschist to eclogite transition; evidence from the Tianshan meta-subduction complex in northwestern China. *Contrib. Mineral. Petrol.* **142,** 1–14.

Garuti G., Zaccarini F., Moloshag V., and Alimov V. (1999) Platinum-group minerals as indicators of sulfur fugacity in ophiolitic upper mantle: an example from chromitites of the Ray-Iz ultramafic complex, Polar Urals, Russia. *Can. Mineral.* **37,** 1099–1115.

Giletti B. J. (1991) Rb and Sr diffusion in alkali feldspars, with implications for cooling histories of rocks. *Geochim. Cosmochim. Acta* **55,** 1331–1343.

Glodny J., Grauert B., Fiala J., Vejnar Z., and Krohe A. (1998) Metapegmatites in the western Bohemian massif: ages of crystallisa-

tion and metamorphic overprint, as constrained by U-Pb zircon, monazite, garnet, columbite and Rb-Sr muscovite data. *Geol. Rundschau.* **87,** 124–134.

Glodny J., Bingen B., Austrheim H., Molina J. F., and Rusin A. (2002) Precise eclogitization ages deduced from Rb/Sr mineral systematics: The Maksyutov complex, Southern Urals, Russia. *Geochim. Cosmochim. Acta* **66,** 1221–1235.

Glodny J., Austrheim H., Montero P., and Rusin A. (1999) The Marun-Keu metamorphic complex, Polar Urals, Russia: Protolith ages, eclogite-facies fluid-rock interaction, and exhumation history. *J. Conf. Abs.* **4(1)** 80.

Gómez-Pugnaire M. T., Karsten L., and López Sánchez-Vizcaíno V. (1997) Phase relationships and P-T conditions of coexisting eclogite-blueschists and their transformation to greenschist-facies rocks in the Nerkau Complex (Northern Urals). *Tectonophys.* **276,** 195–216.

Green P. F., Duddy I. R., Gleadow A. J. W., and Lovering J. F. (1989) Apatite fission-track analysis as a palaeotemperature indicator for hydrocarbon exploration. *Oil & Gas Geol.* **11,** *2,* 156–177.

Hacker B. R. (1996) Eclogite formation and the rheology, buoyancy, seismicity, and H_2O content of oceanic crust. In *Dynamics of Subduction* (eds. G. E. Bebout, D. Scholl, S. Kirby, and J. P. Platt) AGU Monograph, pp. 337–346. Washington, DC 96.

Hamilton W. (1970) The Uralides and the motion of the Russian and Siberian platforms. *Geol. Soc. Am. Bull.* **81,** *9,* 2553–2576.

Heinrich C. A. (1982) Kyanite-eclogite to amphibolite facies evolution of hydrous mafic and pelitic rocks, Adula nappe, Central Alps. *Contrib. Mineral. Petrol.* **81,** 30–38.

Hetzel R. (1999) Geology and geodynamic evolution of the high-P/low-T Maksyutov Complex, southern Urals, Russia. *Geol. Rundsch.* **87,** 577–588.

Holland T. J. B. (1979) High water activities in the generation of high pressure kyanite eclogites of the Tauern window, Austria. *J. Geol.* **87,** 1–27.

Holland T. J. B. and Blundy J. D. (1994) Non-ideal interactions in calcic amphiboles and their bearing on amphibole-plagioclase thermometry. *Contrib. Mineral. Petrol.* **116,** 433–447.

Inger S., Ramsbotham W., Cliff R. A., and Rex D. C. (1996) Metamorphic evolution of the Sesia-Lanzo Zone, Western Alps: time constraints from multi-system geochronology. *Contrib. Mineral. Petrol.* **126,** 152–168.

Ivanov S. N., Perfiliev A. S., Efimov A. A., Smirnov G. A., Necheukhin V. M., and Fershtater G. B. (1975) Fundamental features in the structure and evolution of the Urals. *Am. J. Sci.* **254,** 107–136.

Jamtveit B., Bucher-Nurminen K., and Austrheim H. (1990) Fluid-controlled eclogitization of granulites in deep crustal shear zones, Bergen Arcs, western Norway. *Contrib. Mineral. Petrol.* **104,** 184–193.

Joesten R. (1991) Grain boundary diffusion kinetics in silicate and oxide minerals. In: Diffusion, Atomic ordering and Mass transport: Selected topics in Geochemistry (ed. J. Ganguly). *Adv. Phys. Geochem.* **8,** 345–395.

Johnson C. A. and Harlow G. E. (1999) Guatemala jadeitites and albitites were formed by deuterium-rich serpentinizing fluids deep within a subduction zone. *Geology* **27,** 629–632.

Kelley S. P. and Wartho J. A. (2000) Rapid kimberlite ascent and the significance of Ar-Ar ages in xenolith phlogopites. *Science* **289 (5479),** 609–611.

Klemd R. and Bröcker M. (1999) Fluid influence on mineral reactions in ultrahigh-pressure granites; a case study in the Snieznik Mts. (West Sudetes, Poland). *Contrib. Mineral. Petrol.* **136(4),** 358–373.

Kühn A., Glodny J., Iden K., and Austrheim H. (2000) Retention of Precambrian Rb/Sr phlogopite ages through Caledonian eclogite facies metamorphism, Bergen Arc Complex, W-Norway. *Lithos.* **51,** 305–330.

Laird J. and Albee A. L. (1981) High-pressure metamorphism in mafic schist from northern Vermont. *Am. J. Sci.* **281,** 97–126.

Leech M. L. and Stockli D. F. (2000) The late exhumation history of the ultrahigh-pressure Maksyutov complex, southern Ural mountains, from new apatite fission track data. *Tectonics* **19(1),** 153–167.

Lennykh V. I., Valizer P., and Schulte B. A. (1997) Eclogites and blue schists of Urals; evolution and geodynamics. *Terra Abstr.* **9,** Suppl.1., 17.

Ludwig K. R. (1999) Isoplot/Ex Ver 2.06: A geochronological toolkit for Microsoft Excel. *Berkeley Geochronol. Center Special Publications.* 1a.

Manning C. E. (1998) Fluid composition at the blueschist-eclogite transition in the model system Na_2O-MgO-SiO_2-H_2O-HCl. *Schweiz. Mineral. Petrogr. Mitt.* **78,** 225–242.

Maresch W. V. and Abraham K. (1981) Petrography, mineralogy and metamorphic evolution of an eclogite from the island of Margarita, Venezuela. *J. Petrol.* **22(3),** 337–362.

Markl G. and Bucher K. (1997) Proterozoic eclogites from the Lofoten Islands, Northern Norway. *Lithos.* **42,** 15–35.

Miller C. and Thöni M. (1995) Origin of eclogites from the Austroalpine Ötztal basement (Tirol, Austria): geochemistry and Sm-Nd vs. Rb-Sr isotope systematics. *Chem. Geol.* **122,** 199–225.

Molina J. F., Austrheim H., Glodny J., and Rusin A. (2002) The eclogites of the Marun-Keu Complex (Polar Urals, Russia). *Lithos.* **61,** 55–78.

Mørk M. B. E. (1999) Compositional variations and provenance of Triassic Sandstones from the Barents Shelf. *J. Sed. Res. (A).* **69(3),** 690–710.

Nadeau S., Philippot P., and Pineau F. (1993) Fluid inclusion and mineral isotopic compositions (H-C-O) in eclogitic rocks as tracers of local fluid migration during high-pressure metamorphism. *Earth Planet. Sci. Lett.* **114,** 431–448.

Nakashima S. (1995) Diffusivity of ions in pore water as a quantitative basis for rock deformation rate estimates. *Tectonophys.* **245***(3–4)***,** 185–203.

Philippot P. and Selverstone J. (1991) Trace-element-rich brines in eclogitic veins: implications for fluid composition and transport during subduction. *Contrib. Mineral. Petrol.* **106,** 417–430.

Poli S. (1993) The amphibolite-eclogite transformation; an experimental study on basalt. *Am. J. Sci.* **293***(10)***,** 1061–1107.

Puchkov V. N. (1997) Structure and geodynamics of the Uralian orogen. In *Orogeny through time* (eds. J. P. Burg and M. Ford). *Geol. Soc. London Spec. Publ.* **121,** 201–236.

Rubie D. C. (1986) The catalysis of mineral reactions by water and restrictions on the presence of aqueous fluid during metamorphism. *Min. Mag.* **50,** 399–415.

Rubie D. C. (1990) Role of kinetics in the formation and preservation of eclogites. In *Eclogite facies rocks* (ed. D. A. Carswell), pp. 111–140. Blackie, Glasgow.

Savelieva G. N. and Nesbitt R. W. (1996) A synthesis of the stratigraphic and tectonic setting of the Uralian ophiolites. *J. Geol. Soc. London.* **153,** 525–537.

Scambelluri M. and Philippot P. (2001) Deep fluids in subduction zones. *Lithos.* **55,** 213–227.

Scambelluri M., Pennacchioni G., and Philippot P. (1998) Salt-rich aqueous fluids formed during eclogitization of metabasites in the Alpine continental crust (Austroalpine Mt. Emilius unit, Italian western Aps). *Lithos.* **43,** 151–167.

Selverstone J., Franz G., Thomas S., and Getty S. (1992) Fluid variability in 2 GPa eclogites as an indicator of fluid behaviour during subduction. *Contrib. Mineral. Petrol.* **112,** 341–357.

Seward D., Brown D., Hetzel R., Friberg M., Gerdes A., Petrov G. A., and Perez-Estaun A. (2002) The syn- and post-orogenic low temperature events in the Southern and Middle Uralides: Evidence from fission-track analysis. In: Mountain Building in the Uralides: Pangea to the Present (eds. D. Brown, C. Juhlin, and V. Puchkov). *AGU Geophysical Monograph* **132,** 257–272.

Sharma M., Wasserburg G. J., Papanastassiou D. A., Quick J. E., Sharkov E. V., and Laz′ko E. E. (1995) High $^{143}Nd/^{144}Nd$ in extremely depleted mantle rocks. *Earth Planet. Sci. Lett.* **135,** 101–114.

Shmelev V. R. and Puchkov V. N. (1986) Tectonic features of the Ray-Iz ultramafic massif (Polar Urals). *Geotectonics.* **22(4),** 314–327.

Sneeringer M., Hart S. R., and Shimizu N. (1984) Strontium and samarium diffusion in diopside. *Geochim. Cosmochim. Acta* **48,** 1589–1608.

Sobolev N. V., Dobretsov N. L., Bakirov A. B. and Shatsky V. S. (1986) Eclogites from various types of metamorphic complexes in the USSR and the problems of their origin. In: *Blueschists and eclogites* (eds. B. W. Evans and E. H. Brown). *Memoir— Geological Society of America* **164,** 349–363.

Sobornov K. O. and Rostovshchikov V. (1996) Structure and hydrocarbon prospects of the North Urals thrust belt. *Petrol. Geosci.* **2,** 177–184.

Stöckhert B., Brix M. R., Kleinschrodt R., Hurford A. J., and Wirth R. (1999) Thermochronometry and microstructures of quartz; a comparison with experimental flow laws and predictions on the temperature of the brittle-plastic transition. *J. Struct. Geol.* **21,** 351–369.

Stosch H. G. and Lugmair G. W. (1990) Geochemistry and evolution of MORB-type eclogites from the Münchberg Massif, Southern Germany. *Earth Planet. Sci. Lett.* **99,** 230–249.

Straume A. K. and Austrheim H. (1999) Importance of fracturing during retro-metamorphism of eclogites. *J. Metamorph. Geol.* **17,** 637–652.

Thöni M. and Jagoutz E. (1992) Some new aspects of dating eclogites in orogenic belts: Sm-Nd, Rb-Sr, and Pb-Pb isotopic results from the Austroalpine Saualpe and Koralpe type-locality (Carinthia/Styria, southeastern Austria). *Geochim. Cosmochim. Acta* **56,** 347–368.

Tilton G. R., Ames L., Schertl H. P., and Schreyer W. (1997) Reconaissance isotopic investigations on rocks of an undeformed granite contact within the coesite-bearing unit of the Dora Maira Massif. *Lithos.* **41,** 25–36.

Udovkina N. G. (1971) Eclogites of the Polar Urals. pp. 1–191. Nauka, Moscow.

Veblen D. R. and Buseck P. R. (1981) Hydrous pyriboles and sheet silicates in pyroxenes and uralites: Intergrowth microstructures and reaction mechanisms. *Am. Mineral.* **66,** 1107–1134.

Vernon R. H. (1984) Microgranitoid enclaves in granites—globules of hybrid magma quenched in a plutonic environment. *Nature* **309,** 438–439.

Villa I. M. (1998) Isotopic closure. *Terra Nova.* **10(1),** 42–47.

Widmer T. and Thompson A. B. (2001) Local origin of high pressure vein material in eclogite facies rocks of the Zermatt-Saas Zone, Switzerland. *Am. J. Sci.* **301,** 627–656.

Yardley B. W. D. (1997) The evolution of fluids through the metamorphic cycle. In *Fluid Flow and Transport in Rocks*. (eds. B. Jamtveit and B. W.D. Yardley). pp. 99–117. Chapman & Hall, London.

Yardley B. W. D. and Baltatzis E. (1985) Retrogression of staurolite schists and the sources of infiltrating fluids during metamorphism. *Contrib. Mineral. Petrol.* **89,** 59–68.

Yoder H. S. (1952) The MgO-Al_2O_3-SiO_2-H_2O-system and the related metamorphic facies. *Am. J. Sci.* **250-A,** 569–627.

Zonenshain L. P., Korinevsky V. G., Kazmin V. G., Pechersky D. M., Khain V. V., and Matveenkov V. V. (1984) Plate tectonic model of the South Urals development. *Tectonophys.* **109(1–2),** 95–135.

APPENDIX: SAMPLE DESCRIPTIONS

a) Marun-Keu complex

Partially preserved igneous protolith assemblages

PU 62 (67°29.04′ N, 66°29.61′ E) Coronitic gabbro, showing partial eclogitization. Assemblages: a) Igneous assemblage (mainly coarse-grained): olivine, orthopyroxene (enstatite), diopside, plagioclase, amphibole (?), Cr-spinel, biotite, sulphides, ilmenite. b) Metamorphic assemblage (mainly fine-grained): omphacite, garnet, Ca-amphibole, zoisite/clinozoisite, phengite, Cr-kyanite, quartz, rutile, Cl-apatite, Na-diopside. Magmatic assemblage as cores to corona structures. Metamorphic reaction starts from grain boundaries and cracks, implying fluid availability as reaction-controlling factor.

Eclogite facies veins/shear zones and related prograde metamorphism

J2 (67°29.70′ N, 66°32.01′ E) Quartz-rich eclogite facies vein, in an eclogite wall rock, both showing eclogite-facies vein-parallel foliation. Static recrystallization of the quartz in the vein. Assemblages: a) Vein: quartz, white mica, omphacite, garnet, rutile. b) Eclogite: omphacite, garnet, quartz, white mica, rutile, apatite, zircon.

J13 (67°29.67′ N, 66°32.10′ E) Eclogite facies vein (1 cm width), in garnet amphibolite. Vein shows zonation: white mica-quartz aggregate forms central part of the vein, with seams of omphacitite and garnet-rich lithology. Host rock is slightly weathered. Assemblage vein: omphacite (partly symplectized), quartz, white mica, garnet, rutile.

J21 (67°29.70′ N, 66°32.04 E) Heterogeneous vein fill. Assemblage: omphacite (locally symplectized), rutile (up to 5 cm), white mica (cm-sized), garnet (fine-grained, locally abundant, forming "garnetite"), albite, apatite.

J30/J32 (67°33.68′ N, 66°36.40′ E) Shear zone, made up from strongly foliated felsic (*meta*-granitoid) rock (J30), with ca. 10–15 cm wide eclogite aureola (J32) (Fig. 3, grading into garnet amphibolite. Growth of dendritic amphibole in eclogite aureola. In shear zone: Static quartz recrystallization at high grade conditions. Assemblage J30: quartz, garnet, white mica, amphibole, rutile, epidote/zoisite, apatite, zircon. Assemblage J32: omphacite, amphibole, garnet, rutile, white mica.

Eclogite facies equilibrium assemblages

J12 (67°29.70′ N, 66°32.01′ E) Transition between mafic eclogite and garnet amphibolite. In the field mafic eclogite is in contact to a rutile-bearing quartz-phengite vein. With increasing distance from the vein, three lithologies are distinguished:

J12a: Eclogite, dominated by omphacite and white mica, coarse grained, with strong eclogite facies deformation (preferred orientation of omphacite and white mica). Assemblage: omphacite, phengitic white mica, paragonite, quartz, amphibole (rare), garnet (rare), rutile, apatite, clinozoisite (?), zircon. Transition to J12b as almost sharp contact.

J12b: Eclogite, finer-grained than J12a, without foliation. Assemblage similar to J12a, but amphibole (Na-Ca-amphibole) and garnet are more abundant. Transition to J12c is a diffuse, ca. 2 cm wide zone characterised by increase of amphibole at the expense of omphacite.

J12c: Garnet-amphibolite, without foliation, dominated by Ca-Na-amphibole. Assemblage:, amphibole, garnet, paragonite, phengitic white mica, quartz, rutile, apatite, zircon, cyanite (traces).

J24 (67°28.65′ N, 66°36.13′ E) Leucocratic *meta*-migmatite, coarse-grained, slightly foliated, with compositional layering, intercalated with sample J25. Assemblage: quartz, plagioclase, garnet, white mica, clinozoisite/epidote, amphibole (rare, blue-green), apatite, rutile, zircon.

J25 (67°28.65′ N, 66°36.13′ E) Mesocratic *meta*-migmatite, with compositional layering and eclogite facies foliation (defined by white mica and omphacite). Intercalated with sample J25. Assemblage:, quartz, plagioclase (rare), Ca-amphibole ("dendritic" blasts), omphacite, garnet, clinozoisite/epidote, white mica, apatite, rutile, zircon.

PU55 (67°29.72′ N, 66°31.98′ E) Eclogite. Assemblage: omphacite, garnet, white mica, amphibole, subordinate apatite, quartz, rutile, zircon. Pronounced eclogite facies foliation, with subsequent static growth of dendritic amphibole. Two types of amphibole: a) poikiloblastic-dendritic amphibole, up to 1 cm in size, replacing omphacite, with garnet and phengite inclusions b) amphibole (+ symplectite) as retrogression product of omphacite+garnet, related to a small crack (fluid pathway, Fig. 2c) Retrogression postdates growth of dendritic amphiboles.

PU61 (67°29.72′ N, 66°31.98′ E) Massive, medium-grained biotite-bearing eclogite. Assemblage: omphacite, garnet, biotite, apatite, rutile, pyrite, quartz, amphibole. Equigranular granoblastic-polygonal equilibrium texture, no foliation. No indications for retrograde overprint.

Retrogression (amphibolitization) related veins and retrogressed rocks

J5 (67°29.55′ N, 66°32.01′ E) plagioclase-dominated metamorphic vein. No deformation. In places development of "graphic granite." Associated fluids cause amphibolitization of host rock eclogites. Assemblage: plagioclase, quartz, white mica (up to 10 cm in size), epidote.

PU10a (67°34.71′ N, 66°38.80′ E) Metagranite, coarse-grained, slightly foliated. Mineral association: quartz, plagioclase, K-feldspar (reddish), biotite, garnet (rare), apatite, white mica, ilmenite, magnetite, epidote, zircon, sphene. Metamorphic conditions of latest equilibration probably amphibolite facies (presence of sphene instead of rutile). Indications for slight greenschist facies overprint.

PU12 (67°34.85′ N, 66°39.92′ E) Metagranite. Mineralogy suggests latest equilibration at amphibolite facies. Slight diaphthoritic overprint (probably greenschist facies). No foliation. Mineral association: quartz, plagioclase, K-feldspar, biotite, garnet, white mica, ilmenite, amphibole, epidote, allanite, apatite, zircon, rutile, sphene, rare relics of omphacite.

J22 (67°28.65′ N, 66°36.13′ E) Feldspar-dominated vein. (Fig. 2d)

Fluids caused wallrock amphibolitization. Assemblage: feldspar (macro-perthitic, "moonstone"), amphibole, clinozoisite/epidote, white mica, quartz. Outcrop situation: Amphibolitization haloes around veins are proportional to vein thickness.

PU31 (67°33.44′ N, 66°37.04′ E) Sample with ca. 10 cm wide transition zone from eclogite (equilibrated, fine-grained, eclogite facies ductile deformation restricted to an only ca. 1 cm wide shear zone related to a small quartz-rich vein) to garnet amphibolite. Garnet amphibolite statically replaces the eclogite facies assemblage. Replacement reactions starting along microfractures and grain boundaries.

a) eclogite facies assemblage: garnet, omphacite, white mica, apatite, epidote, rutile, quartz, amphibole. b) garnet-amphibolite mineral association: garnet, amphibole, plagioclase, epidote, white mica, quartz, sphene, apatite; relics: omphacite, rutile.

Amphibolite- to greenschist-facies overprint

PU32 (67°33.44′ N, 66°37.04′ E) Biotite eclogite, slightly retrogressed. Mineral association: omphacite, garnet, amphibole, biotite, albite. Incipient breakdown of omphacite (to symplectite) and biotite (to chlorite)

b) Rai-iz ophiolite complex

PU4 (66°58′ N, 65°33′ E) Vein in ultramafic rocks of the Rai-Iz massif. Vein assemblage: plagioclase (oligoclase), amphibole, phlogopite, corundum (ruby, some in gemstone quality), chromite, apatite. Host rock: Dunite-Serpentinite with chromite layers. Fluids caused serpentinization and remobilized Cr.